



**HAL**  
open science

## **AOP and IATA applied to ocular surface toxicity**

Noémie Bonneau, Christophe Baudouin, Annabelle Reaux-Le Goazigo,  
Françoise Brignole-Baudouin

► **To cite this version:**

Noémie Bonneau, Christophe Baudouin, Annabelle Reaux-Le Goazigo, Françoise Brignole-Baudouin. AOP and IATA applied to ocular surface toxicity. *Regulatory Toxicology and Pharmacology*, 2021, 125, pp.105021. 10.1016/j.yrtph.2021.105021 . hal-03474463

**HAL Id: hal-03474463**

**<https://hal.sorbonne-universite.fr/hal-03474463>**

Submitted on 10 Dec 2021

**HAL** is a multi-disciplinary open access archive for the deposit and dissemination of scientific research documents, whether they are published or not. The documents may come from teaching and research institutions in France or abroad, or from public or private research centers.

L'archive ouverte pluridisciplinaire **HAL**, est destinée au dépôt et à la diffusion de documents scientifiques de niveau recherche, publiés ou non, émanant des établissements d'enseignement et de recherche français ou étrangers, des laboratoires publics ou privés.

## **REVIEW**

### **An Overview of Current Alternative Models in the Context of Ocular Surface Toxicity**

Noémie Bonneau <sup>a,b,\*</sup>, Christophe Baudouin<sup>a,c,d</sup>, Annabelle Reaux-Le Goazigo<sup>a</sup>, Françoise Brignole-Baudouin<sup>a,c,e</sup>

<sup>a</sup> Sorbonne Université, INSERM, CNRS, IHU FOReSight, Institut de la Vision, 75012 Paris, France

<sup>b</sup> Horus Pharma, 06700 Saint-Laurent-du-Var, France

<sup>c</sup> Centre Hospitalier National d'Ophtalmologie des Quinze-Vingts, INSERM-DGOS CIC 1423, IHU FOReSight, 75012, France

<sup>d</sup> Université Versailles-Saint-Quentin-en-Yvelines, Hôpital Ambroise Paré, APHP, F-92100 Boulogne-Billancourt, France

<sup>e</sup> Université de Paris, Faculté de Pharmacie de Paris, 75006 Paris, France

\* Correspondence: [noemie.bonneau@inserm.fr](mailto:noemie.bonneau@inserm.fr) (N. Bonneau)

### **Abstract**

The 21<sup>st</sup> century has seen a steadily increasing social awareness of animal suffering, with increased attention to ethical considerations. Developing new integrated approaches to testing and assessment (IATA) strategies is an Organisation for Economic Co-operation and Development (OECD) goal to reduce animal testing. Currently, there is a lack of alternative models to test for ocular surface toxicity (aside from irritation) in lieu of the Draize eye irritation test (OECD guideline No. 405) performed in rabbits. Five alternative *in vitro* or *ex vivo* methods have been validated to replace this reference test, but only in combination. However, pathologies like Toxicity-Induced Dry Eye (TIDE), cataract, glaucoma and neuropathic pain can occur after exposure to a pharmaceutical product or chemical and therefore need to be anticipated. To do so, new models of lacrimal glands, lens, neurons innervating epithelia are required. These models must take into account real life exposure (dose, time, and tear film clearance). The scientific community is working hard to develop new, robust, alternative, *in silico* and *in vitro* models, while attempting to balance ethics and availability of biological materials. This review provides a broad overview of the validated methods for analysing ocular irritation and those still used by some industries, as well as promising models that need to be optimized according to the OECD. Finally, we give an

34 overview of recently developed innovative models which could become new tools in the  
35 evaluation of ocular surface toxicity within the scope of IATAs.

36

### 37 **Short abstract**

38 Until now, the Draize test in rabbits has been the only test performed to anticipate ocular  
39 toxicity of pharmaceutical compounds, mainly irritation. However, in the field of alternative  
40 approaches, new models must be developed and validated. This review aims to give an  
41 overview of the OECD validated methods and of innovative models, which could become  
42 new tools in the evaluation of ocular surface toxicity.

43

44

45 **Key words:** Draize Eye Test; OECD guidelines; Ocular Surface; In Silico; 3D Multicellular;  
46 Cornea-on-a-chip; Organoids

47

48

### 49 **Introduction**

50 Since the beginning of the 21<sup>st</sup> century, modern toxicology has been focusing on the 3R  
51 principle, “Reduce, Refine, Replace”, established in 1959 by Russell and Burch, stipulating  
52 that the use of laboratory animals should be only a last resort. Since 2013, in Europe, the  
53 cosmetic industry has been confronted with strict prohibition of evaluating its products on  
54 animals. Integrated approaches of testing and assessment (IATA), promoted by the OECD  
55 (Organisation for Economic Cooperation and Development) might enable validation of new  
56 compounds in this sector (Canavez *et al.* 2021).

57 To date, validated alternative models have been available only for the evaluation of potential  
58 ocular surface irritation. Models to predict Toxicity-Induced Dry Eye (TIDE), anterior  
59 segment neuropathies or other ocular surface changes are still in the stage of basic science  
60 research. Furthermore, classification of ocular irritants is based on the United Nations  
61 Organization (UNO) system, *i.e.* the GHS “Globally Harmonized System of Classification  
62 and Labelling of Chemicals” (Luechtefeld *et al.* 2016). This international system  
63 distinguishes severe irritants (Category 1), moderate irritants (Category 2A), mild irritants  
64 (Category 2B) and non-irritants (No Category). However, unlike the Draize test, the *in vivo*  
65 reference model in rabbits, current alternative models for ocular irritation cannot distinguish  
66 Category 2A from 2B irritants. These irritants are usually differentiated based on the kinetics

67 of the reversibility of damage. Of note, the lack of reproducibility of the *in vivo* test of  
68 reference, the Draize test, complicates the validation of alternative models by the ICCVAM  
69 (Interagency Coordinating Committee on the Validation of Alternative Methods)(OECD  
70 Webinar 2019a).

71 In its first section, this review presents updates in the latest methodology for evaluation of  
72 ocular irritation, first presenting the five *in vitro* or *ex vivo* models validated by the OECD, in  
73 combination, to replace the Draize test (Guideline (GL) 405)(OECD, 2020a): Reconstructed  
74 human Cornea-like Epithelium (RhCE) viability tests (GL 492)(OECD, 2019a), Bovine  
75 Corneal Opacity and Permeability (BCOP) test (GL 437)(OECD, 2020b), Isolated Chicken  
76 Eye (ICE) test (GL 438)(OECD, 2018a), Fluorescein Leakage (GL 460)(OECD, 2017), and  
77 Short Time Exposure assay (STE, GL 491)(OECD, 2020c). The ocular irritation IATA  
78 indicates the combination of tests that should be considered depending on whether the product  
79 is suspected to be an irritant ('top-down' approach) or is thought to be in the non-irritant  
80 category ('bottom-up' approach). This review also presents models used by some cosmetic  
81 companies that either were or still are under evaluation by the OECD, such as the Isolated  
82 Rabbit Eye (IRE) test, Hen's Egg Test on the Chorio-Allantoic Membrane (HET-CAM).  
83 Characteristics and protocol details of the models for ocular irritation are summarized in  
84 Table I.

85 Next, promising models mentioned in the OECD Guidance Document No. 263 (OECD,  
86 2019b) are presented. These models, if optimized and validated, might represent a major asset  
87 in classifying new compounds into Categories 2A and 2B: PorCORA (Porcine Ocular Cornea  
88 Opacity/Reversibility Assay), EVEIT (Ex Vivo Eye Irritation Test), 3D Hemi-Cornea and  
89 SMI (Slug Mucosal Irritation assay).

90 Finally, in order to prevent complex toxicities as TIDE, glaucoma, cataract, some of which  
91 are rare topical side effects, new models presented in the literature could be validated and  
92 incorporated into new IATAs, taking into account real-life exposure, pharmacokinetics and  
93 knowledge already reported in the literature. Therefore, this final section provides an  
94 overview of *in silico* and *in vitro* models which could, in combination, enable complete  
95 evaluation of ocular surface toxicities within the framework of IATAs.

96

## 97 **Alternative models to the Draize test according to OECD GL 405**

98

99 *Reconstructed human Cornea-like Epithelium (RhCE)*

100 Since the last update of GL 492 in 2019 (OECD, 2019a), four models of RhCE are now  
101 available to evaluate ocular surface irritation, two of which are considered Validated  
102 Reference Methods (VRM): EpiOcular™ (VRM1), SkinEthic™ HCE (VRM2), LabCyte  
103 CORNEA-MODEL24 and MCTT HCE™. These RhCE models mimic human corneal  
104 epithelium morphologically, histologically, biochemically and physiologically and can be  
105 used first in a ‘bottom-up’ approach to identify non-irritant substances. Even though cellular  
106 damage can occur through several mechanisms, only cytotoxicity measurements are carried  
107 out. Indeed, cell viability is considered to be proportional to the severity of damage and  
108 representative of the global response of the ocular surface: mild irritants with low transcorneal  
109 penetration alter only the superficial corneal epithelium, whereas moderate or severe irritants  
110 can penetrate more deeply, reaching the corneal stroma and sometimes endothelium. This  
111 global response would be a correct representation of the damage that could occur in humans  
112 after toxic exposure, no matter the cellular mechanisms involved, ranging from slight  
113 conjunctival erythema or edema to severe changes such as corneal opacification.

114 While there may be differences between RhCE models (Table II), mainly concerning the cell  
115 types used and duration of epithelium culture, the testing method is similar: direct application  
116 of the tested compounds on the 3D epithelium and viability cytotoxicity assays reflecting the  
117 mitochondrial metabolic ability of viable cells. If corneal viability diminishes to below the  
118 fixed threshold (specific to each RhCE, see Table II), this will suggest classification of the  
119 compound as an ocular irritant. Above the threshold, the compound will not be classified and  
120 must be combined with another validated GL (437, 438, 460, 491 or in last option, if the test  
121 compound is not a cosmetic, GL 405 *i.e.* Draize test). Nevertheless, the OECD Guidance  
122 Document No. 263 (OECD, 2019b) reports the ongoing OECD evaluation of the EpiOcular™  
123 time-to-toxicity (ET<sub>50</sub>) assay, a test that could enable the differentiation of category 2A from  
124 2B irritants (Kandarova *et al.* 2018). This new protocol is based on multiple time and  
125 concentration exposures. It could represent a major asset in the scope of IATA decision trees,  
126 since as of yet, no validated alternative model alone can distinguish between all the categories  
127 of irritants.

128 Another limitation is that GL 492 can only be used for solids, semi-solids, liquids and waxes,  
129 since gases and aerosols have not undergone validation procedures. Nonetheless, this aspect  
130 should be investigated, since many accidental ocular exposures are caused by volatile  
131 compounds (OECD 2019a).

132

133 *Bovine Corneal Opacity and Permeability assay (BCOP)*

134 Recommended as the first step of a ‘top-down’ strategy, the organotypic BCOP model  
135 described in GL 437 (OECD, 2020b) enables differentiation between severe irritants applied  
136 to isolated bovine cornea from slaughterhouses. It can also identify non-irritants in a ‘bottom-  
137 up’ approach. The eyeballs are kept *ex vivo* for a brief period, during which physiological and  
138 biochemical functions remain unaltered. After excision, corneas are anchored on a corneal  
139 holder composed of two chambers, both filled with preservation medium. Briefly, the  
140 endothelial surface of the cornea is placed on the *o-ring* in the posterior chamber, while the  
141 epithelial surface is positioned in the anterior chamber.

142 Two application methods, adapted to the type of compound being tested, are described in the  
143 GL, but an important parameter is verification that the product covers the entire epithelial  
144 surface and that the washing step is sufficient to retrieve all of the compound. Irritancy  
145 potential is then measured through the *In Vitro* Irritancy Score (IVIS), which combines the  
146 diminution of light transmission capacity (corneal opacity, measured with an opacimeter) and  
147 the increase in fluorescein sodium passage (permeability, *i.e.* the amount of dye dropped in  
148 the anterior chamber and that crosses the corneal thickness). Of note, fluorescein sodium is an  
149 anionic compound, not retained by a healthy, negatively charged epithelium. A substance will  
150 be categorized as a severe irritant if the IVIS is greater than 55 and as a non-irritant if the  
151 IVIS is less than 3. However, if the IVIS is between 3 and 55, additional tests will be required  
152 to distinguish category 2 irritants. It is also possible to complement these results with a  
153 histologic analysis of the cornea, which procedure is described in the Guidance Document No.  
154 160 (OECD, 2018b).

155 Of note, since the last guideline update in June 2020, a second opacimeter can be used  
156 (LLBO), requiring adaptation of the IVIS equation and decision criteria, but the performance  
157 is comparable to OP-KIT, the first opacimeter validated.

158

159 *Isolated Chicken Eye (ICE)*

160 Like the BCOP model, the ICE aims to discriminate Category 1 GHS substances in a ‘top-  
161 down’ strategy but can also be included in a ‘bottom-up’ approach to identify non-irritants.  
162 The ICE is regulated by OECD GL 438, last updated in 2018 (OECD, 2018a). This test uses  
163 enucleated eyes of chickens for human consumption. In this assay, corneas are not excised.  
164 The whole eye is placed in a stainless-steel clamp with the cornea positioned vertically. The  
165 clamp is placed in a superfusion chamber to nourish the cornea. At the start of the test, the

166 clamp is retrieved from the chamber and the cornea positioned horizontally in order to apply  
167 the tested compounds. A qualitative and quantitative evaluation of the cornea is conducted to  
168 establish potential opacities, epithelial morphological alterations (detected by fluorescein  
169 sodium retention) and edema. As for BCOP, corneal opacity and fluorescein retention are  
170 scored, and are associated to a morphological evaluation which is “subjective according to the  
171 interpretation of the investigator” (GL 438). The combination of these scores enables the GHS  
172 classification of test compounds. For instance, with three scores of I, the substance is  
173 considered a non-irritant.

174 Furthermore, since the last GL update, histological features after paraffin embedding can be  
175 analyzed notably for detergents and surfactant irritants (OECD, 2019b). Indeed, there should  
176 be a correlation between erosion, vacuole formation in the inferior area of the epithelium,  
177 presence of pycnotic nuclei and irreversibility of the damage. GL 438 proposes another table  
178 to score those parameters.

179

#### 180 *Fluorescein Leakage (FL)*

181 The FL test follows GL 460 (OECD, 2017). The FL method is performed *in vitro* on a semi-  
182 permeable membrane (insert) leading to a single-layer culture of renal tubular cells of Madin-  
183 Darby Canin (MDCK CB997). This is a well described cell line, known to form tight  
184 junctions and desmosomes. Its organization is similar to the non-proliferative apical corneal  
185 epithelium. Furthermore, permeabilization of corneal epithelium is known to be one of the  
186 first phenomena occurring in toxicity-induced ocular irritation.

187 Changes in tight junctions and desmosomes are proportional to the quantity of fluorescein  
188 sodium that diffuses into the basal chamber, evaluated through FL<sub>20%</sub>, that is to say the  
189 concentration of the tested compound that leads to an FL of 20% compared to negative  
190 controls (single layer of cells not exposed and insert without cells). The substance tested is  
191 categorized as a severe irritant on the GHS ocular irritation classification if the  $FL_{20\%} \leq 100$   
192 mg/mL.

193 Integrated into a ‘top-down’ strategy, this simple method enables distinguishing Category 1  
194 chemicals without additional data. However, unlike the previous methods presented, this  
195 method can only be used with water-soluble compounds or mixtures. Indeed, solids in  
196 suspension will precipitate. In addition, it is not applicable to strong bases or acids, volatile  
197 compounds or cellular fixatives, because the toxic mechanisms for these types of compounds  
198 (such as protein coagulation or saponification) cannot be evaluated by FL. Finally, colored or

199 viscous compounds should be tested with other methods, since their complete washout  
200 required before the fluorescent measurement is complicated. Of note, a compound with a  
201 strong affinity for the insert membrane can lead to the same problem. Therefore, this affinity  
202 must be tested, as described in the GL, before beginning the assay. While reversibility of the  
203 epithelial changes cannot yet be evaluated, this will be considered in the next update of the  
204 GL, with the possibility of using FL to separate Categories 2A and 2B of the GHS  
205 classification.

206

#### 207 *Short Time Exposure Assay (STE)*

208 The STE, GL 491 (OECD, 2020c), can be considered in ‘bottom-up’ and ‘top-down’  
209 strategies. STE enables the evaluation of all types of chemicals except volatile compounds  
210 with a vapor pressure above 6 kPa<sup>1</sup> and solid non-surfactants (not water-soluble after at least 5  
211 min in NaCl). This *in vitro* model consists of a confluent monolayer culture of rabbit corneal  
212 fibroblasts (several cell lines are possible, such as CCL60 or SIRC). If cell viability (MTT  
213 assay, see Table 2) is less than 70% with both concentrations, the substance is placed in  
214 Category 1 without any additional assay. If cell viability is above 70% with at least one  
215 concentration, additional tests are required.

216

#### 217 **Other ocular irritation models evaluated by the OECD**

218

##### 219 *Vitrigel-Eye Irritancy Test (EIT) method*

220 While not mentioned in GL 405 as an alternative method, the OECD introduces this method  
221 in its Guidance Document n°263 (OECD, 2019b) and in the 2019 GL 494 (OECD, 2019c),  
222 establishing the protocol for the Vitrigel EIT method. This method can be used only in a  
223 ‘bottom-up’ approach to identify non-irritants. It evaluates the barrier function of a human  
224 corneal epithelium reconstructed on a Vitrigel matrix (ECh-T immortalized cell line ; collagen  
225 gel obtained by rehydration of a hydrogel that has undergone a vitrification  
226 process)(Takezawa *et al.* 2004; Yamaguchi *et al.* 2016) with a Transepithelial Electrical  
227 Resistance (TEER) measurement. Of note, this ohmmeter analysis is sensitive to the number  
228 of cell passages and to room temperature (Srinivasan *et al.* 2015). This measurement is  
229 characterized by three parameters: time lag, intensity and plateau level. A non-irritant product  
230 is identified by a time lag > 180 seconds, an intensity < 0.05% and a plateau level ≤ 5.0%. If  
231 one of these criteria differs, additional studies are required to classify the product. A



232 limitation of this method is its small range of application, being limited to liquids or semi-  
233 liquids with a pH > 5. However, unlike previous methods described, it can be used for volatile  
234 compounds and products that interfere with the detection of formazan in the MTT assay.

235

#### 236 *Ocular Irritection*<sup>®</sup>

237 Ocular Irritection<sup>®</sup> is an *in vitro* macromolecular test which is the subject of a GL drafted in  
238 2019 (OECD, 2019d). It is suitable either in a ‘bottom-up’ or ‘top-down’ strategy for solids  
239 and liquids with a pH between 4 and 9. It is an acellular system composed of proteins,  
240 glycoproteins, carbohydrates, lipids and low molecular weight compounds. Ocular  
241 Irritection<sup>®</sup> test aims to mimic the organized and transparent structure of the cornea after  
242 rehydration (Eskes *et al.* 2014). This enables specific detection of protein coagulation or lipid  
243 saponification mechanisms. Nevertheless, since the system is devoid of cells, cytotoxicity  
244 cannot be evaluated. The matrix and the testing principle are presented in figure 1. Any  
245 change in the matrix organization leads to a modification of the turbidity and reflects the  
246 irritative capacity of the test compound. However, like many alternative models, this testing  
247 method alone is unable to distinguish mild irritants.

248

#### 249 *Cytosensor Microphysiometer (CM)*

250 Because of the lack of commercial availability of the Cytosensor Microphysiometer  
251 technology, the preliminary GL version released in 2012 (OECD, 2012) for the evaluation of  
252 water-soluble compounds, solids, viscous substances or homogenous suspensions has seen its  
253 development discontinued in 2016 (European Commission 2020a). Nevertheless, it could be  
254 integrated into a ‘bottom-up’ or ‘top-down’ approach if similar instruments were to come to  
255 market. It consists of an adherent, confluent, single layer of mice fibroblasts (cell line L929)  
256 cultured on a polycarbonate insert. These cells are designed to represent conjunctival and  
257 corneal epithelia. The test endpoint is the Metabolic Rate Decrement of 50% (MRD<sub>50</sub>), that is  
258 to say the concentration that reduces the acidification rate by 50%. This measurement reveals  
259 irritation potential, since damaged cells will produce less acidic metabolites in the culture  
260 medium. On the one hand, if the MRD<sub>50</sub> ≤ 2 mg/mL, the product is considered to be a severe  
261 irritant in a ‘top-down’ approach. On the other hand, if the MRD<sub>50</sub> > 10 mg/mL, the test  
262 compound is classified as a non-irritant in a ‘bottom-up’ strategy. Of note, the GL mentions  
263 that this testing method could evaluate reversibility if optimized.

264

#### 265 *Neutral Red Release (NRR)*

266 The NRR test evaluates cytotoxicity on a single layer fibroblast or keratinocyte culture loaded  
267 with neutral red 3 hours before the exposure to test compounds (OECD, 2019b). This vital  
268 dye incorporates itself into lysosomes of viable cells. Several protocols have been proposed in  
269 the literature (Zuang 2001), such as the FRAME protocol based on mice embryonic  
270 fibroblasts (3T3-L1 cell line) or the *Clonetics Corporation* protocol using human  
271 keratinocytes. In both cases, the endpoint is the NRR<sub>50</sub>, that is to say the test compound  
272 concentration that releases, in the culture medium, 50% of the neutral red incorporated by  
273 lysosomes. The more toxic a substance is, the more cellular membranes, including lysosomal  
274 membranes, are altered, leading to leakage of intracellular compounds such as neutral red.  
275 Validated by internal procedures in many industries, the ICCVAM is requesting  
276 supplementary data on inter-laboratory reproducibility before publishing a GL on the Neutral  
277 Red Release assay (OECD, 2019b). It is also being considered for use in combination with the  
278 EpiOcular time-to-toxicity assay on RhCE.

279

#### 280 *Red Blood Cell test (RBC)*

281 The RBC test evaluates the ability of test compounds to disrupt red cell membranes (relation  
282 between hemolysis and oxyhemoglobin denaturation) and in this way, to classify products  
283 into GHS Categories 1 or non-classified (OECD, 2019b). RBC test can be conducted on red  
284 blood cells from various species (pig, sheep, rabbit) (Lewis *et al.* 1993; Mehling *et al.* 2007;  
285 Pape *et al.* 1987; Pape 1990). The irritant potential score corresponds to the ratio between the  
286 leakage of red blood cell hemoglobin in the supernatant (H<sub>50</sub> concentration inducing a red cell  
287 hemolysis of 50%) and oxyhemoglobin (denaturation index, DI). If H<sub>50</sub>/DI > 100, the  
288 substance is considered a non-irritant, between 10 and 100 the substance is categorized as a  
289 mild irritant (Category 2), between 1-10 as a moderate irritant, and if the H<sub>50</sub>/DI < 1, the  
290 compound is classified in Category 1 (severe irritant).

291 An application of this method on 12 shampoos and 7 conditioners was proposed by Alves *et*  
292 *al.* (2008), attesting to a 91.6% sensitivity and 100% specificity of the method. However, in  
293 the Guidance Document n°263 (OECD, 2019b), the OECD underscores the necessity for  
294 more data on the types of compound that can be tested, in other words, the method's range of  
295 application. Indeed, while the literature reports other studies on surfactants, mixtures  
296 (Mehling *et al.* 2007) and eyedrops (Martins *et al.* 2012), the chemical and physical properties  
297 of test compounds must be further investigated.

298

299 *Isolated Rabbit Eye (IRE)*

300 Although the IRE test is similar to the ICE (compound exposure time, endpoints ; see Table  
301 1), this organotypic model on the enucleated rabbit eye has not been validated by the  
302 ICCVAM since its 2010 evaluation, due to the lack of a standardized protocol, the lack of  
303 data on decision criteria, and the fact that rabbit eyes come from experimental animals and not  
304 from slaughterhouses as with BCOP or ICE (Lee *et al.* 2017; Prinsen and Koëter 1993).  
305 Nevertheless, the IRE is accepted in the European Union for distinguishing severe irritants  
306 (except alcohols, solids and surfactants, for which there are too many false negatives)  
307 (ICCVAM 2010).

308

309 *Hen's Egg Test on Chorioallantoic Membrane (HET-CAM)*

310 The HET-CAM is an alternative model developed by Luepke in 1985 and modified to classify  
311 irritant compounds. Indeed, the chorioallantoic membrane of the egg is considered to be a  
312 reasonable facsimile of the conjunctiva and its vasculature. Of note, from this model was  
313 derived another model, the Chorioallantoic Membrane Vascular Assay (CAMVA). The main  
314 nuance between the two (see figure 2) could enable differentiation of non-irritants from mild  
315 or moderate irritants.

316 The main advantages of using embryonated eggs are their accessibility, low cost and rapid  
317 growth. These eggs can be kept in an incubator for up to 13 days of maturation. After 14 days  
318 of growth, the development of the embryo is advanced, and the model is then considered an *in*  
319 *vivo* model (Kue *et al.* 2015).

320 While the ICCVAM did not validate this testing method for distinguishing severe irritants  
321 (ICCVAM 2010), this method is still used by some industrials in their internal weight of  
322 evidence WoE, these methods being recognized in the European Union. The procedure for  
323 opening the eggs without breaking the vascular membrane is described in figure 2.

324 However, one should bear in mind that this testing method has been increasingly criticized,  
325 being considered an *in vivo* model even in the first days of embryonic development.

326

327 **Models requiring optimization according to the OECD**

328

329 The models introduced in the following section are models mentioned in the OECD Guidance  
330 Document n°263 as interesting models, if optimized, for evaluation of reversibility of ocular

331 irritation/corrosion, which may thus be able to distinguish between all GHS categories,  
332 including category 2 compounds.

333

#### 334 *Porcine Ocular Cornea Opacity/Reversibility Assay (PorCORA)*

335 PorCORA is an organotypic model similar to BCOP, since it is based on the maintenance *ex*  
336 *vivo* of porcine cornea obtained from slaughterhouses. Its added value lies in the air interface  
337 preservation allowing maintenance for 21 days (same as in the Draize reference test, the  
338 amount of time needed to evaluate reversibility of damage). Several steps are required to  
339 prepare the excised corneas (Vij *et al.* 2017). First, the corneas are placed in a 24-well plate,  
340 with the epithelium facing the bottom of the well. A mixture of agar/gelatin/medium is poured  
341 onto the corneas, which are then placed in Petri dishes after gelification. The test compounds  
342 are applied directly to the corneal surface (10  $\mu$ L for liquids, 20 mg for solids) for 5 minutes.  
343 The corneas are then washed with PBS (Piehl *et al.* 2011). Corneal alterations and their  
344 reversibility are then estimated and scored based on the area of staining with fluorescein  
345 sodium over the course of 1, 2, 3, 7, 10, 14 and 21 days after compound exposure (European  
346 Commission 2020b).

347 In this way, Piehl *et al.* demonstrated in 2011 that this method gave similar results to the  
348 Draize reference test (correlation coefficient of 0.98) with reproducible results for the five  
349 control test substances: phosphate buffered saline (PBS), absolute ethanol (EtOH), 3%  
350 sodium dodecyl sulfate (SDS), 1% benzalkonium chloride (BAK), and 10% sodium  
351 hydroxide (NaOH). Furthermore, in this study, PorCORA identified reversible and  
352 irreversible effects. By establishing a PorCORA score, it could be possible to distinguish  
353 GHS category 1 products (irreversible alterations before 21 days) from category 2 products  
354 (reversible damages before 21 days, with a score returning to 0).

355 Nevertheless, additional data is needed. Indeed, in this study, Piehl *et al.* found that the  
356 method was too sensitive for surfactants. Similarly, in another study conducted on shampoos  
357 and hair dyes, PorCORA overestimated the irritant potential (Donahue *et al.* 2011). Finally, a  
358 drawback of this model is the progressive opacification of the cornea due to the gel that  
359 prevents the endothelium from correctly regulating corneal stromal fluids (Spöler *et al.* 2015).

360

#### 361 *Ex Vivo Eye Irritation Test (EVEIT)*

362 The EVEIT is an air-liquid interface culture system, enabling maintenance of excised rabbit  
363 corneas (from slaughterhouses) for 72 hours following compound application. Briefly,  
364 corneas with a scleral ring are removed and anchored in a chamber filled with a minimal

365 volume of medium to maintain hydrostatic pressure. This *ex vivo* model reflects the  
366 biochemical activity of corneal epithelium and endothelium. Its advantage compared to the  
367 PorCORA system presented above is that the EVEIT does not lead to corneal opacification  
368 during culture (Spöler *et al.* 2015). Decision criteria are evaluated four times over 72 hours  
369 enabling differentiation of non-irritants from category 2A irritants (OECD, 2019b; Spöler *et*  
370 *al.* 2015): macroscopic observation of corneal opacity, fluorescein sodium diffusion, corneal  
371 thickness and structural changes measured by optical coherence tomography. Each  
372 measurement results in a score, similar to those used in the ICE or Draize tests, which were  
373 described by Spöler *et al.* in 2015. If preservation time of the corneas *ex vivo* could be  
374 improved, this testing method could enable differentiation of all category 2 products. Of note,  
375 this method was used by Schrage *et al.* in 2012 to evaluate the effect of artificial tears on  
376 corneal epithelial repair after mechanical damage. This study highlights the fact that the  
377 models presented in this section could serve equally well for toxicity studies as for  
378 pharmacological studies for the development of ophthalmic treatments.

379

### 380 *3D Hemi-Cornea*

381 The first *in vitro* system that may potentially discriminate GHS categories 1 and 2 alone, the  
382 3D Hemi-Cornea combines, in an insert, a corneal human epithelium reconstituted from an  
383 immortalized cell line with human corneal immortalized keratinocytes which represent  
384 stromal cells (Bartok *et al.* 2015; Engelke *et al.* 2013; Zorn-Kruppa *et al.* 2014). The two cell  
385 types are separated by a collagen membrane allowing evaluation of the two cell lines  
386 independently after a 60 min-exposure of the chemical (Zorn-Kruppa *et al.* 2014). This model  
387 is adapted for liquids as well as solids but is constraining since it has to be cultured during 7  
388 days with a daily change of medium. The endpoint measured is metabolic activity and the  
389 cytotoxicity MTT test. The distinction between GHS categories non-irritant, 1 and 2 could be  
390 observed though the extension and/or localisation of corneal changes (Tandon *et al.* 2015).  
391 Moderate irritants lead to a loss of viability of the corneal epithelium and can affect the  
392 stroma, whereas severe irritants lead to severe corneal epithelial and stromal alterations. As a  
393 result, this system properly classifies category 1 compounds and 80% of category 2  
394 compounds, but only 50% of non-irritant substances, with an overestimation of their irritant  
395 potential. A hypothesis to explain these last, disappointing results is that the compounds in  
396 this category were frequently viscous and difficult to remove during the washing steps,  
397 leading to the deterioration of some epithelial layers (Bartok *et al.* 2015). Furthermore, in

398 another study, the irritation potential of compounds with extreme pH were again  
399 overestimated, as in other *in vitro* tests, possibly because of the absence of the mucinous layer  
400 of the tear film, which has a buffer effect *in vivo* (Zorn-Kruppa *et al.* 2014).

401 Nonetheless, this test quoted in the Guidance Document n°263 of OECD seems to be an  
402 option for the evaluation of surfactants, alcohols, ketones, and volatile compounds, in other  
403 words, compounds that, in many other alternative models, lead to false positives results. This  
404 3D hemi-cornea could at the same time allow the evaluation of compound diffusion, since the  
405 test substances need to cross an aqueous collagen membrane.

406

#### 407 *Slug Mucosal Irritation (SMI) assay*

408 Described in the literature for the evaluation of reversible or irreversible ocular (Lenoir *et al.*  
409 2011a) and nasal (Lenoir *et al.* 2013) stinging, itching and/or burning (SIB), the SMI test  
410 measures the liberation of mucus proteins from *Arion lusitanicus* slugs. This method can  
411 screen for ocular discomfort generated by isolated ingredients or final products. As presented  
412 in the schematic protocol Figure 3, the slug's weight is compared before and after every  
413 contact period (CP)(Lenoir *et al.* 2009, 2011a, 2013; Cutuli *et al.* 2021).

414 Developed by Lenoir *et al.*, this test was used to evaluate shampoos and artificial tears. The  
415 results were correlated with a clinical study (Spearman's Rank correlation of 0.986,  $p <$   
416 0.001)(Lenoir *et al.* 2011b). Similarly, Petit *et al.* 2017 was able to reproduce this alternative  
417 model in 2017 to evaluate veterinary products. Recently, a new SMI alternative model, using  
418 a "Yellow slug", was reported to evaluate surface disinfectants used against SARS-CoV-2  
419 (Cutuli *et al.* 2021).

420 Since it can distinguish category 2 irritant products, optimization and validation of this test is  
421 mentioned to be of interest in the OECD Guidance Document n°263. However, depending on  
422 national regulations, this test might be considered animal experimentation (OECD, 2019b).

423

#### 424 **New innovative models for ocular surface toxicity evaluation**

425

426 Mimicking ocular structures *in vitro* is challenging (lacrimal glands, conjunctiva, innervation,  
427 lens, ...). New models are being developed in basic science research, notably using fluidic  
428 and three-dimensional approaches. These technologies of organ-on-a-chip originate from the  
429 area of pharmaceutical research and development (Wilson *et al.* 2015). In addition, this  
430 review will focus on *in silico* approaches, which are required to understand real-life exposure

431 and thus aid in design of the *in vitro* strategy, reducing time and costs of development.  
432 Organoid models will be described in the final part of this section, even though these new  
433 cellular structures are mainly studied for the purpose of replacing deficient patient structures.  
434 Table III proposes an overview of the selected models.

435

#### 436 *In silico models*

437 *In silico* approaches, using computer and mathematical tools, aim to simulate *in vivo*  
438 biological processes, mimicking a multicellular organ crossed by biological flows and  
439 connected to other structures of the organism. Inspired by the “PB-PK”, *Physiologically*  
440 *Based Pharmacokinetics*, approach (predicting absorption, distribution, metabolism and  
441 elimination), these *in silico* methods try to improve toxicological evaluation, taking into  
442 account local metabolism, barriers, ..., and to estimate a toxic dose (Knudsen *et al.* 2015).  
443 Once the organ is modelled, multiple scenarios can be tested by changing dose, time, method  
444 of exposure and other parameters that could influence the risk of toxicity (for instance,  
445 enzyme polymorphisms, pregnant women or pediatric differences in metabolism)(Jones *et al.*  
446 2015).

447 For each product tested, an exhaustive knowledge of its physicochemical properties must  
448 come through computerized channels (Brochot *et al.* 2014). To this end, other *in silico* tools  
449 can contribute to the information in the literature: *Qualitative and Quantitative Structure*  
450 *Activity Relationship* (QSAR) models that can predict biological properties such as affinity,  
451 protein binding, based on chemical structure. These models are available as free access or  
452 commercial software (ECHA 2019). To encourage regulatory acceptance of these QSAR  
453 models, the OECD released Guidance Document n°69 and created a free access toolbox with  
454 some QSAR models (OECD 2020d). First developed for conception of possible  
455 pharmaceuticals, some QSAR models aim to predict ocular irritation and damage based on the  
456 compound’s toxicodynamic properties: acidity, electrophilicity, chemical reactivity, surfactant  
457 effect (OECD, 2019b). For instance, Kulkarni *et al.* (2001) examined membrane interactions  
458 of compounds with the stratified lipophilic corneal epithelium to determine the irritant  
459 potential of substances already classified by the Draize test *in vivo*.

460 For local ocular toxicity, it is essential to mimic three main factors that influence ocular  
461 surface penetration and distribution: static barriers with different transport systems (claudins,  
462 zonula occludens), dynamic clearance (lacrimal fluids, Schlemm’s canal drainage) and  
463 metabolic factors (enzymes, efflux pumps, receptors). In 2018, Pak *et al.* applied these

464 principles to develop an *in silico* rabbit cornea model (epithelium, stroma, endothelium), the  
465 Quasi-3D CoBi (Computational Biology) model which includes passive transport  
466 (paracellular, transcellular) through the corneal epithelium (barrier to the passage of  
467 hydrophilic compounds), transport through the stroma (barrier to the passage of lipophilic  
468 compounds) and protein binding (such as glycosaminoglycans which can retain hydrophilic  
469 compounds). To do so, the research team created a precise geometric representation of the  
470 multilamellar corneal structure, applying complex mathematic equations to reflect the various  
471 flows. Nevertheless, this *in silico* model should be elaborated by adding all of the ocular  
472 structures (such as conjunctiva, tear film, neurons, retina) and should be based on human data  
473 to improve the predictions made through these models. The lack of human data on barriers,  
474 thickness and porosity of layers, local metabolism, physical constants, ..., remains to this day  
475 a barrier to the development of *in silico* models and use as a high throughput tool.  
476 Implementation of this work would be extremely time-consuming and would require a great  
477 deal of computing power but would improve extrapolations.

478 By enabling the identification of target structures, these models could guide the first steps of  
479 the AOP (adverse outcome pathway), which are currently the subject of toxicological  
480 development as supports for implantation of IATA, limiting unnecessary *in vitro* studies.  
481 However, one should bear in mind that if an important metabolic pathway used by the  
482 compound tested is missed in the model, the predictions will not be accurate.

483

#### 484 *3D multicellular models*

485 Numerous 3D models are described in the literature, improving the phenotype of the  
486 epithelium formed. Nevertheless, many of them neglect the tear film, which covers the  
487 epithelia of the ocular surface, as well as the innervation of the ocular surface, which are,  
488 however, two central structures in understanding and anticipating TIDE and anterior segment  
489 neuropathies. Thus, this section describes three models that could become assets in the  
490 development of IATAs for ocular surface toxicity: the first model presented would allow  
491 evaluation of tear film thickness and composition, while the following ones would permit  
492 analysis of the toxic impact on neurons interacting with corneal cells.

493

#### 494 - Conjunctiva and lacrimal gland coculture

495 The literature is rich in alternative corneal models but delves less into conjunctival and  
496 lacrimal gland toxicity, although these structures which are essential for production of the tear



497 film, a fundamental structure to be evaluated for the anticipation of TIDE. Nevertheless, in  
498 2017, Lu *et al.* proposed a coculture between rabbit primary epithelial conjunctival cells and  
499 spheroids of rabbit primary lacrimal acinar cells. To our knowledge, this is the first *in vitro*  
500 3D model capable of producing aqueous and mucinous layers of the tear film.

501 After testing several configurations, direct contact between the two cell types, as presented  
502 figure 4, was found to present the best configuration, with optimal epithelial morphology,  
503 permeability, phenotype and lacrimal fluid production, even though direct contact is not the  
504 most physiological configuration (no direct contact in humans between these types of cells).  
505 To highlight the usefulness of their model, they demonstrated the protective effect of  
506 dexamethasone, a corticosteroid known to reduce inflammation of the ocular surface in TIDE,  
507 after exposure to pro-inflammatory IL-1 $\beta$ . This effect could not be seen on a simple  
508 monoculture of conjunctival cells. While this model does not allow the formation of a  
509 complete tear film with a lipid layer, it remains an interesting advance for the *in vitro*  
510 anticipation of TIDE. Further studies could be conducted by adding meibocytes in the culture,  
511 to obtain a complete tear film.

512

#### 513 - 3D model of nerve-stroma interactions

514 To date, only a few models consider corneal innervation in a toxic response. Sharif *et al.*  
515 (2018) explored the corneal stroma-neuron interaction in depth by proposing a 3D coculture  
516 on an insert between HCF (*human primary corneal fibroblasts*) and SH-SY5Y neurons, a  
517 well-characterized human neuroblastoma cell line derived from bone marrow. This model is  
518 based on the *de novo* production of extracellular matrix by fibroblast cells and tries to mimic  
519 the *in vivo* nerve-stroma interaction in the cornea, improving the comprehension and  
520 anticipation of corneal cell damage as well as pathways of neuronal regeneration.

521 However, further studies are needed to characterize the neuronal phenotype of this model and  
522 therefore the ability of this model to mimic toxicity affecting the ocular surface. Indeed, SH-  
523 SY5Y neurons do not have the same phenotype as primary sensory neurons from trigeminal  
524 nerves, the main innervation of the ocular surface (Mélik-Parsadaniantz *et al.* 2018), since  
525 they can develop two distinct phenotypes (neuroblastic or epithelial-like). SH-SY5Y includes  
526 adherent cells but also floating viable cells whose biological significance is not yet  
527 understood. Also, neuroblastic SH-SY5Y cells express tyrosine hydroxylase and dopamine- $\beta$ -  
528 hydroxylase, two catecholaminergic markers, which are not characteristic of trigeminal  
529 neurons, which are primarily sensory neurons (Kovalevich and Langford 2013).

530 Nevertheless, transfected SH-SY5Y could be considered to study certain ocular surface  
531 symptoms such as stinging or itching. This was the objective of the NociOcular test based on  
532 a 2D model of SH-SY5Y expressing the transient receptor potential cation channel subfamily  
533 V member TRPV1, known to be implicated in these ocular surface phenomena (Dua *et al.*  
534 2018). Using this test, Forsby *et al.* (2012) completed an ocular tolerability study of 19  
535 shampoos, resulting in only one false negative and two false positives compared to a clinical  
536 evaluation. NociOcular measures, by fluorescence, the intracellular calcium flux mediated by  
537 the activation of TRPV1 and correlated to ocular discomfort. A similar study was conducted  
538 by Narda *et al.* in 2019) on the ocular tolerance of sunscreens, confirming the need to evaluate  
539 disturbances in neuronal transmission and not just damage to the ocular surface epithelial cell  
540 in a comprehensive study.

541

542 - Triculture of neuronal, epithelial and stromal cells

543 Wang *et al.* 2017 proposed an air liquid interface (ALI) triculture between human primary  
544 corneal cells, human corneal stromal stem cells and Chicken Dorsal Root Ganglion (DRG)  
545 neurons, supported by silk proteins. The use of silk proteins aims to mimic the mechanical  
546 properties of the cornea, so as to favour neuronal development. Figure 5 explains the cellular  
547 organization of the model. Through this set up, Wang *et al.* obtained optimized axonal  
548 development as well as a better epithelium / stromal phenotype and viability. At the moment,  
549 corneal tissue models are limited to one or two weeks of culture and do not include the  
550 nervous component. This ALI culture, integrating corneal interactions with neurons while  
551 conserving its integrity for 28 days, enables to evaluate toxic induced alterations of phenotype  
552 and viability. This model represents a progress in tissue engineering, promoting the  
553 importance of cell types interactions for better differentiation and maturation.

554

555 *Cornea-On-a-Chip models*

556 The focus of much attention in recent decades, organs-on-a-chip seek to miniaturize an organ,  
557 facilitate the assembly of cell types and recreate the dynamics of an organ (Mandenius 2018).  
558 These chips are mainly based on microfluidic technics, using biocompatible polymers such as  
559 polydimethylsiloxane (PDMS), a transparent, flexible and gas impermeable organomineral  
560 material. The advantage of these systems lies in the small amount of biological material  
561 needed, while improving the representation of dynamic *in vivo* parameters compared to a  
562 classic 2D cell culture. Nevertheless, protocols have not yet been standardized, scale-up

563 remains unfeasible for routine experimentation, and the analytical challenge (because of the  
564 small quantity of cells) remains to be solved (Sosa-Hernández *et al.* 2018).

565 Because of the complexity of multicompartmental and multi-layered ocular structures,  
566 establishing an eye-on-a-chip is a hard task. If we focus on the anterior segment, some  
567 corneas-on-a-chip are described in the literature and attempt to include ocular surface flow  
568 (blinking of the eyelids, tear secretion, shear stress). Furthermore, microfluidics and  
569 compartmentalization on a chip are also being considered to improve the mimicry of ocular  
570 surface innervation, taking into account the fact that only nerve endings can be directly  
571 exposed to a topically applied toxicant.

572

573 - Cornea-on-a-chip, ocular flows and shear stress

574 A current limitation of corneal barrier models is the lack of flow to mimic the shear stress  
575 caused on the epithelium by eyelid blinking, which is responsible for tear film movement, and  
576 as a result of drug or toxicant distribution and its effects on the ocular surface. Of note, this is  
577 also a limitation of the Draize test when attempting to most closely approximate human  
578 physiology, since rabbits blink less frequently than humans, resulting in a longer exposure  
579 time (Maurice 1995).

580 In 2018, to study passage through the corneal barrier, Bennet *et al.* 2018 proposed a cornea-  
581 on-a-chip with a pulsatile flow to represent blinking or a continuous flow for tear secretion. A  
582 confluent epithelium of 5 to 7 layers with a stable phenotype and permeability was obtained  
583 on a PDMS chip with a fibronectin coated membrane (mimicking Bowman's layer) and  
584 immortalized human corneal epithelial cells. In this system, eyedrop pharmacokinetics and  
585 toxicity can be evaluated by applying either the continuous or pulsatile flow for 5 hours. After  
586 this experimentation time, 98% of the compounds were found to be eliminated; compared to a  
587 static model, it improves the evaluation of absorption, bioavailability and toxicity.  
588 Nevertheless, additional studies are required to understand the impact of the two types of  
589 flow, since compound penetration appeared more significant with the pulsatile flow.

590 Similarly in 2020, Abdalkader and Kamei published a four chamber microfluidic model with  
591 uni- and bi-directional flow to study the impact of shear stress on corneal epithelium barrier  
592 phenotype. This PDMS system, composed of human corneal epithelial cells on a porous  
593 membrane, aims to simulate human cornea, with an apical side in contact with lacrimal fluid  
594 (bidirectional flow for eye blinking) and a proximal side with the aqueous humor  
595 (unidirectional flow mimicking drainage through Schlemm's canal). After having obtained a

596 stratified (2-3 layers), permeable (evaluation by fluorescein diffusion), phenotyped  
597 (expression of tight junction proteins such as the zonula occludens proteins), they applied  
598 both flows for 24 hours and observed that shear stress did not alter cellular adhesion and  
599 improved the expression of cytokeratins, which are important proteins for flexibility, cellular  
600 elasticity and maintaining corneal barrier integrity. In addition, this model could take into  
601 account the compound real time of remanence in the tissue.

602 Nevertheless, these two models are limited in their representation of the cornea, since they  
603 lack formation of the stromal and endothelial layers, corneal elements that are notably  
604 essential for aqueous humor flow. This limitation is addressed by Bai *et al.* (2020) with their  
605 cornea-on-a-chip, a PDMS compartmentalized chip using primary murine corneas; they  
606 simultaneously isolate both epithelial and endothelial corneal cells and plant them into two  
607 separate compartments with a collagen membrane to mimic Bowman's layer.

608

609 - Cornea and conjunctiva-on-a-chip

610 Another approach to the 3D ocular model on-a-chip was designed in 2019 by Seo *et al.*,  
611 combining human primary corneal epithelial cells and immortalized conjunctival cells  
612 (epithelial and glandular cells), cultured in an ALI system. The primary corneal cells are  
613 incorporated into a collagen matrix which mimics the stromal layer. A perfusion system  
614 mimics tear flow, while a biomimetic system recreates blinking of the eyelids. Their  
615 complementary data gives a better representation of this complex model. Seo *et al.* obtained a  
616 pluristratified epithelium with 7 to 8 layers like human cornea, expressing specific markers  
617 (*ex.* cytokeratins 3, 19) and producing a "tear film" of 6  $\mu\text{m}$  comparable to the *in vivo*  
618 thickness. Like the previous models, they proved that shear stress induced cellular  
619 differentiation and limited pro-inflammatory cytokine production. To attest to the utility of  
620 their model, they demonstrated the anti-inflammatory action of lubricin, a protein-like mucin.  
621 While this model does not include the vasculature or immune cells normally present in the  
622 conjunctiva nor the nerve endings of the ocular surface which participate in tear secretion, this  
623 chip represents a major improvement for pharmacological and toxicological compound  
624 evaluation, especially for a TIDE IATA.

625

626 - Corneal innervation compartmentalization

627 Currently, most ocular surface models, like the flow systems just discussed, neglect toxic  
628 effects on ocular surface innervation, whereas during a toxic exposure, trigeminal nerve

629 endings can be altered, with an indirect impact on neuronal cell bodies. Therefore, stimulating  
630 primary cell cultures of neurons directly does not mimic real life exposure, and, as a result,  
631 mechanisms of toxicity are impossible to analyze properly. In order to improve anatomical  
632 representation of the ocular surface innervation, Sarkar *et al.* (2012) used a Campenot device  
633 to evaluate morphological alterations (neurite fragmentation, axon breaks, lack of  
634 regeneration) of mice primary trigeminal neurons after exposition to BAK, preservative  
635 contained in many eyedrops. With this model, they highlighted a dose-dependent toxicity of  
636 BAK on neurites. Campenot devices were the first systems to allow neuronal  
637 compartmentalization but new microfluidic organ-on-a-chip devices could be considered.  
638 Indeed, these microchips can be precisely designed to optimized axonal guidance of  
639 trigeminal neurons (Courte *et al.* 2018). This innovative system also allows to analyze  
640 separately nerve ending and cell body responses. Finally, this model could be improved by  
641 adding corneal epithelial cells in the distal compartment to allow interaction between these  
642 cells and the nerve endings, coming even closer to corneal physiology. It could provide a  
643 better understanding of toxic mechanisms and facilitate establishment of TIDE AOPs and  
644 screening of new therapeutic agents (anti-inflammatory, axonal regeneration,  
645 neuroprotection). Nevertheless, a limitation of this model is the use of primary murine cells,  
646 which does not entirely respect the 3R rule to “Reduce, Replace, Refine,” central in IATA  
647 development. Even if primary cells are a better representation of a peripheral neuronal  
648 phenotype, in the framework of alternative methods, induced Pluripotent Stem Cells should  
649 be considered, as in the organoid models described below.

650

### 651 *Organoid models of the anterior segment of the eye*

652 While the definition can vary between authors, organoids are 3D structures, derived from  
653 embryonic stems cells or induced Pluripotent Stem Cells (iPs), capable of self-organization on  
654 their framework (such as porous membrane and hydrogel) (Duboule 2019). A Pubmed search  
655 with “eye organoid” as keywords reports mostly retinal organoids or organoids destined to be  
656 transplanted in humans to replace deficient structures. Few articles address anterior segment  
657 organoids for *in vitro* evaluation of pathologic or toxic pathways. However, some of the  
658 organoids described could be adapted for toxicological studies.

659

660 - Corneal organoids

661 In 2017, Foster *et al.* presented a corneal organoid derived from an IMR90.4 iPSC cell line  
662 (Foster *et al.* 2017) and published their precise methodology in 2020 (Foster *et al.* 2020).  
663 Mature transparent organoids are obtained after 120 days of cellular sequential selection,  
664 forced aggregation and differentiation. Their lamellar structure is composed of epithelial,  
665 stromal and endothelial layers and expresses specific corneal markers (cytokeratins 3, 14,  
666 collagen of type I, V, VII). Even if any toxicological study has already been conducted, this  
667 model could be further optimized to evaluate the impact of toxic compounds on the  
668 interactions between the three main corneal layers (epithelium, stroma, and endothelium).  
669 Nevertheless, cell differentiation sometimes appears incomplete, leading to the presence of  
670 some retinal cells within the corneal organoid. Other protocols presented to obtain corneal  
671 organoids for transplantation seem to result in pure corneal organoids, such as that of  
672 Susaimanickam *et al.* (2017), but additional studies are needed to evaluate the reproducibility  
673 of these models.

674

#### 675 - Lens organoids

676 In 2018, Murphy *et al.* addressed the unsolved problem of obtaining pure lens cells from  
677 human embryonic pluripotent stem cells (CA-1 cell line). Their objective was to elaborate a  
678 simple, reproducible method to study lens pathologies and anticipate toxicity-induced  
679 cataracts. To this end, they put in place a complex, semi-automated selection protocol based  
680 on knowledge of embryonic development, with successive inhibition and activation of the  
681 FGF, TGF- $\beta$  and Wnt pathways (Yang *et al.* 2010) and magnetic selection of ROR1+  
682 expressing cells (orphan receptor expressed on epithelial lens cells). These organoids remain  
683 viable for 42 days, expressing, among others,  $\alpha$  and  $\beta$  crystallins, present *in vivo* in lens fibers  
684 and necessary for focusing of light. In this study, they proved the ability of these microlenses  
685 to evaluate the toxic potential of a drug candidate, Vx-770, tested in 2016 for cystic fibrosis.  
686 This compound, which has induced toxic cataracts in rats, also altered the lens organoids'  
687 ability to focus light. To summarize, after reproducibility and intra-laboratory transferability  
688 is addressed, this innovative model could be used routinely for the evaluation of mechanisms  
689 of toxicity-induced cataract, which still remain poorly understood, as well as the efficacy of  
690 new treatments.

691

## 692 **Conclusion**

693 The 21<sup>st</sup> century has seen an increase in the movement toward alternative methods to animal  
694 testing, especially since the complete ban of animal experimentation in cosmetics. Ocular  
695 toxicity studies are no exception, and studies still need to be conducted for new compounds.  
696 Indeed, the alternative models to the Draize reference test present similar disadvantages,  
697 among which figure the absence of detection of conjunctival or iris damage, the absence of  
698 evaluation of systemic toxicity that can occur after ocular exposure and the possibility of false  
699 negatives or false positives. Furthermore, none of them alone is able to identify all of the GHS  
700 ocular irritant categories, and reversibility of damage is still difficult to evaluate, explaining  
701 the impetus of the OECD to optimize some other models. In recent decades, toxicology  
702 procedures have aimed to develop IATAs to circumvent these limitations of the alternative  
703 methods. Putting aside Draize reference test, known for its lack of reproducibility which  
704 complexifies the validation of alternative models by the ICCVAM (OECD Webinar 2019a),  
705 and constructing new models, from scratch, based on established AOPs, might be necessary to  
706 improve the robustness of the toxicology approaches and results for human use. Indeed, we  
707 need to break free from Draize eye irritation test and its poor quality of result to improve  
708 inter-laboratory validation of new models (Spielmann 2014) that could enable the  
709 identification of a new category of compounds, very low irritants, which requires finer  
710 sensitivity methods. This validation step is essential to develop robust alternative approaches  
711 to animal testing in the ocular surface field, as it has been done for skin sensitization. Indeed,  
712 in June 2021, OECD released GL 497 on “Defined Approaches for Skin Sensitisation”,  
713 describing the integrated testing strategy and combination of tests that can be used in  
714 toxicology studies in replacement of the reference test on rabbits, the Local Lymph Node  
715 Assay (OECD 2021).

716 In the field of ophthalmology, IATAs should extend the assessment of toxicity to pathologies  
717 other than irritation, especially Toxicity-Induced Dry Eye (TIDE), that can occur after chronic  
718 exposure to very low concentrations (Bonneau *et al.* in press). While much less frequent, a  
719 toxic compound can also lead to, cataract, glaucoma or ocular surface neuropathies after local  
720 exposure. These effects should be considered, taking into account real-life exposure to the  
721 compound, determined through literature searches and *in silico* models. As a result, new  
722 drugs, cosmetic compounds, or other chemicals, should be investigated for acute irritation  
723 and/or for chronic adverse events, depending on real-life use, requiring the development and  
724 validation of models and tests with short and/or repeated exposures.

725 Establishing integrated decision trees for these newly considered adverse events will require a  
726 precise understanding of toxic mechanisms, with the development of Adverse Outcome  
727 Pathways (AOP), a concept also promoted by the OECD with the establishment of new  
728 collaborative tools such as AOP wiki, Effectopedia and the e.AOP.Portal (OECD Webinar  
729 2019b). The innovative models presented in the last section of this review could, after  
730 assessment of robustness and regulatory validation, be included in IATAs. They could be a  
731 key asset to understanding molecular mechanisms and establishing AOPs. Validation of new  
732 models will be a lengthy process, since they should be developed in such a way as to be as  
733 cost-effective and least constraining as possible (ethics and supply logistics).

734

### 735 **Disclosures of Conflicts of Interests**

736 CB is consultant for Aerie, Alcon, Allergan, Horus Pharma, Santen and Théa.

737 CB and FBB has received research grants from Horus Pharma, Santen and Théa.

738 NB has received funding from Horus Pharma and *l'Agence Nationale de la Recherche et de la*  
739 *Technologie* (ANRT) through a *Convention Industrielle de Formation par la Recherche*  
740 (CIFRE).

741

### 742 **Acknowledgment**

743 The authors thank Dr Kevin CLARK, MD, for checking and editing the manuscript.

744

### 745 **References**

746 Abdalkader, R. & Kamei, K.I. (2020). Multi-corneal barrier-on-a-chip to recapitulate eye  
747 blinking shear stress forces. *Lab on a Chip*, 20(8):1410-1417. doi: 10.1039/c9lc01256g.

748 Alves, EN., Presgrave, Rde. F., Presgrave, O.A., Sabagh, F.P., de Freitas, J.C., & Corrado,  
749 A.P. (2008). A reassessment of the in vitro RBC haemolysis assay with defibrinated  
750 sheep blood for the determination of the ocular irritation potential of cosmetic products:  
751 comparison with the in vivo Draize rabbit test. *Alternative to Laboratory Animals*,  
752 36(3):275-84. doi: 10.1177/026119290803600305.

753 Bai, J., Fu, H., Bazinet, L., Birsner, A.E., & D'Amato, R.J. (2020). A Method for Developing  
754 Novel 3D Cornea-on-a-Chip Using Primary Murine Corneal Epithelial and Endothelial  
755 Cells. *Frontiers in Pharmacology*, 11:453. doi: 10.3389/fphar.2020.00453.

756 Bartok, M., Gabel, D., Zorn-Kruppa, M., & Engelke, M. (2015). Development of an in vitro  
757 ocular test system for the prediction of all three GHS categories. *Toxicology In Vitro*,  
758 29(1):72-80. doi: 10.1016/j.tiv.2014.09.005.

759 Bennet, D., Estlack, Z., Reid, T., & Kim, J. (2018). A microengineered human corneal  
760 epithelium-on-a-chip for eye drops mass transport evaluation. *Lab on a Chip*,  
761 18(11):1539-1551. doi: 10.1039/c8lc00158h.



762 Bonneau, N., Baudouin, C., & Brignole-Baudouin, F. (in press). AOP and IATA applied to  
763 ocular surface toxicity. *Regulatory Pharmacology and Toxicology*.

764 Brochot, C., Willemin, M.E., & Zeman, F. (2014). *Chapter 13. Modelisation Toxicopharmacokinetic with Physiological Basis: Role for risk and pharmacology evaluation*.  
765 French (Material ed.). Franck Varenne Publishing Company.

767 Canavez, A.D.P.M., Corrêa, G.O.P, Isaac, V.L.B., Schuck, D.C., & Lorencini, M. (2021).  
768 Integrated approaches to testing and assessment as a tool for the hazard assessment and  
769 risk characterization of cosmetic preservatives. *Journal of Applied Toxicology*, 1-13. doi:  
770 10.1002/jat.4156.

771 Courte, J., Renault, R., Jan, A., Viovy, J.L., Peyrin, J.M., & Villard, C. (2018).  
772 Reconstruction of directed neuronal networks in a microfluidic device with asymmetric  
773 microchannels. *Methods in Cell Biology*, 148:71-95. doi: 10.1016/bs.mcb.2018.07.002.

774 Cutuli, M.A., Guarnieri, A., Pietrangelo, L., Magnifico, I., Venditti, N., Recchia, L., ...  
775 Petronio, G. (2021). Potential Mucosal Irritation Discrimination of Surface Disinfectants  
776 Employed against SARS-CoV-2 by *Limacus flavus* Slug Mucosal Irritation Assay.  
777 *Biomedicines*, 9(4):424. doi: 10.3390/biomedicines9040424.

778 Donahue, D.A., Avalos, J., Kaufman, L.E., Simion, F.A., & Cerven, D.R. (2011). Ocular  
779 irritation reversibility assessment for personal care products using a porcine corneal  
780 culture assay. *Toxicology In Vitro*, 25(3):708-14. doi: 10.1016/j.tiv.2010.12.008.

781 Dua, H.S., Said, D.G., Messmer, E.M., Rolando, M., Benitez-Del-Castillo, J.M., Hossain,  
782 P.N., ... Baudouin, C. (2018). Neurotrophic keratopathy. *Progress in Retinal Eye  
783 Research*, 66:107-131. doi: 10.1016/j.preteyeres.2018.04.003.

784 Duboule, D.(2019). *Organoids, Embryoids: From 3D cultures to development and  
785 pathological models* French. [Internet][cited 2020 Apr 21]. Available from:  
786 [https://www.college-de-france.fr/media/denis-  
787 duboule/UPL4053860021427582586\\_CdF.2019.cours1.pdf](https://www.college-de-france.fr/media/denis-duboule/UPL4053860021427582586_CdF.2019.cours1.pdf)

788 ECHA (European Chemicals Agency) (2019). *Modèles QSAR*. [Internet][cited 2020 Apr 22].  
789 Available from: [https://echa.europa.eu/fr/support/registration/how-to-avoid-unnecessary-  
790 testing-on-animals/qsar-models](https://echa.europa.eu/fr/support/registration/how-to-avoid-unnecessary-testing-on-animals/qsar-models)

791 Engelke, M., Zorn-Kruppa, M., Gabel, D., Reisinger, K., Rusche, B., & Mewes, K.R. (2013).  
792 A human hemi-cornea model for eye irritation testing: quality control of production,  
793 reliability and predictive capacity. *Toxicology In Vitro*, 27(1):458-68. doi:  
794 10.1016/j.tiv.2012.07.011.

795 Eskes, C., Hoffmann, S., Facchini, D., Ulmer, R., Wang, A., Flego, M., ... Wilt, N. (2014).  
796 Validation study on the Ocular Irritation assay for eye irritation testing. *Toxicology In  
797 Vitro*, 28(5):1046-65. doi: 10.1016/j.tiv.2014.02.009.

798 European Commission (2020a). *The Cytosensor Microphysiometer Toxicity Test*.  
799 [Internet][cited 2020 Apr 10]. Available from: [https://tsar.jrc.ec.europa.eu/test-  
800 method/tm2004-01](https://tsar.jrc.ec.europa.eu/test-method/tm2004-01)

801 European Commission (2020b). *Porcine Corneal Opacity Reversibility Assay*. [Internet][cited  
802 2020 Apr 13]. Available from: <https://tsar.jrc.ec.europa.eu/test-method/tm2008-03>

803 Forsby, A., Norman, K.G., El Andaloussi-Lilja, J., Lundqvist, J., Walczak, V., Curren, R., ...  
804 Tierney, N.K. (2012). Using novel in vitro NociOcular assay based on TRPV1 channel  
805 activation for prediction of eye sting potential of baby shampoos. *Toxicological*

806 *Sciences, 129* (2):325-31. doi: 10.1093/toxsci/kfs198.

807 Foster, J.W., Wahlin, K., Adams, S.M., Birk, D.E., Zack, D.J., & Chakravarti, S. (2017).  
808 Cornea organoids from human induced pluripotent stem cells. *Scientific*  
809 *Reports*, 7:41286. doi: 10.1038/srep41286.

810 Foster, J.W., Wahlin, K.J., & Chakravarti, S. (2020). A Guide to the Development of Human  
811 Cornea Organoids from Induced Pluripotent Stem Cells in Culture. *Methods in*  
812 *Molecular Biology*, 2145:51-58. doi: 10.1007/978-1-0716-0599-8\_5.

813 ICCVAM (2010). *Test Method Evaluation Report: Current Validation Status of In Vitro Test*  
814 *Methods Proposed for Identifying Eye Injury Hazard Potential of Chemicals and*  
815 *Products (Volume 2) Interagency Coordinating Committee on the Validation of*  
816 *Alternative Methods National Toxicology Program Interagency Center for the*  
817 *Evaluation of Alternative Toxicological Methods*. [Internet][cited 2020 Apr 9]. Available  
818 from: [https://ntp.niehs.nih.gov/iccvam/docs/ocutox\\_docs/invitro-2010/tmer-vol2.pdf](https://ntp.niehs.nih.gov/iccvam/docs/ocutox_docs/invitro-2010/tmer-vol2.pdf)

819 Jones, H.M., Chen, Y., Gibson, C., Heimbach, T., Parrott, N., Peters, S.A., ... Hall, S.D.  
820 (2015). Physiologically based pharmacokinetic modeling in drug discovery and  
821 development: a pharmaceutical industry perspective. *Clinical Pharmacology &*  
822 *Therapeutics*, 97(3):247-62. doi: 10.1002/cpt.37.

823 Kandarova, H., Letasiova, S., Adriaens, E., Guest, R., Willoughby, J.A.Sr., Drzewiecka, A.,  
824 ... Van Rompay, A.R. (2018). CON4EI: CONSortium for in vitro Eye Irritation testing  
825 strategy - EpiOcular™ time-to-toxicity (EpiOcular ET-50) protocols for hazard  
826 identification and labelling of eye irritating chemicals. *Toxicology In Vitro*, 49:34-52.  
827 doi: 10.1016/j.tiv.2017.08.019.

828 Knudsen, T.B., Keller, D.A., Sander, M., Carney, E.W., Doerrer, N.G., Eaton, D.L., ...  
829 Whelan, M. (2015). FutureTox II: in vitro data and in silico models for predictive  
830 toxicology. *Toxicological Sciences*, 143(2):256-67. doi: 10.1093/toxsci/kfu234.

831 Kovalevich, J., & Langford, D. (2013). Considerations for the use of SH-SY5Y  
832 neuroblastoma cells in neurobiology. *Methods in Molecular Biology*, 1078:9-21. doi:  
833 10.1007/978-1-62703-640-5\_2.

834 Kue, C.S., Tan, K.Y., Lam, M.L., & Lee, H.B. (2015). Chick embryo chorioallantoic  
835 membrane (CAM): an alternative predictive model in acute toxicological studies for anti-  
836 cancer drugs. *Experimental Animals*, 64(2):129-38. doi: 10.1538/expanim.14-0059.

837 Kulkarni, A., Hopfinger, A.J., Osborne, R., Bruner, L.H., & Thompson, E.D. (2001).  
838 Prediction of eye irritation from organic chemicals using membrane-interaction QSAR  
839 analysis. *Toxicological Sciences*, 59(2):335-45. doi: 10.1093/toxsci/59.2.335.

840 Lee, M., Hwang, J.H., & Lim, K.M. (2017). Alternatives to In Vivo Draize Rabbit Eye and  
841 Skin Irritation Tests with a Focus on 3D Reconstructed Human Cornea-Like Epithelium  
842 and Epidermis Models. *Toxicological Research*, 33(3):191-203. doi:  
843 10.5487/TR.2017.33.3.191.

844 Lenoir, J., Adriaens, E., & Remon, J.P. (2009). *A New Application of the Slug Mucosal*  
845 *Irritation (SMI) Assay: Detecting Nasal Stinging, Itching and Burning (SIB)*. Paper  
846 presented at the 7th World Congress on Alternatives and Animal Use in the Life  
847 Sciences, Rome, Italy.

848 Lenoir, J., Adriaens, E., & Remon, J.P. (2011a). New aspects of the Slug Mucosal Irritation  
849 assay: predicting nasal stinging, itching and burning sensations. *Journal of Applied*  
850 *Toxicology*, 31(7):640-8. doi: 10.1002/jat.1610.

- 851 Lenoir, J., Claerhout, I., Kestelyn, P., Klomp, A., Remon, J.P., & Adriaens, E. (2011b). The  
852 slug mucosal irritation (SMI) assay: development of a screening tool for the evaluation  
853 of ocular discomfort caused by shampoos. *Toxicology In Vitro*, 25(8):1919-25. doi:  
854 10.1016/j.tiv.2011.06.009.
- 855 Lenoir, J., Bachert, C., Remon, J.P., & Adriaens, E. (2013). The Slug Mucosal Irritation  
856 (SMI) assay: a tool for the evaluation of nasal discomfort. *Toxicology In Vitro*,  
857 27(6):1954-61. doi: 10.1016/j.tiv.2013.06.018.
- 858 Lewis, R.W., McCall, J.C., & Botham, P.A. (1993). A comparison of two cytotoxicity tests  
859 for predicting the ocular irritancy of surfactants. *Toxicology In Vitro*, 7(2):155-8. doi:  
860 10.1016/0887-2333(93)90126-p.
- 861 Lu, Q., Yin, H., Grant, M.P., & Elisseff, J.H. (2017). An In Vitro Model for the Ocular  
862 Surface and Tear Film System. *Scientific Reports*, 7(1):6163. doi: 10.1038/s41598-017-  
863 06369-8.
- 864 Luechtefeld, T., Maertens, A., Russo, D.P., Rovida, C., Zhu, H., & Hartung, T. (2016).  
865 Analysis of Draize eye irritation testing and its prediction by mining publicly available  
866 2008-2014 REACH data. *ALTEX*, 33(2):123-34. doi: 10.14573/altex.1510053.
- 867 Luepke, N.P. (1985). Hen's egg chorioallantoic membrane test for irritation potential. *Food  
868 and Chemical Toxicology*, 23(2):287-91. doi: 10.1016/0278-6915(85)90030-4.
- 869 Mandenius, C.F. (2018). Conceptual Design of Micro-Bioreactors and Organ-on-Chips for  
870 Studies of Cell Cultures. *Bioengineering (Basel)*, 5(3):56.  
871 doi:10.3390/bioengineering5030056.
- 872 Martins, D.N.A., Alves E.N., Presgrave, Rde.F., Costa, R.N., & Delgado, I.F. (2012).  
873 Determination of Eye Irritation Potential of Low-Irritant Products: Comparison of in  
874 Vitro Results with the in Vivo Draize Rabbit Test. *Brazilian Archives of Biology and  
875 Technology*, 55(3):381-88.
- 876 Maurice, D. (1995). The effect of the low blink rate in rabbits on topical drug penetration.  
877 *Journal of Ocular Pharmacology and Therapeutics*, 11(3):297-304. doi:  
878 10.1089/jop.1995.11.297.
- 879 Mehling, A., Kleber, M., & Hensen, H. (2007). Comparative studies on the ocular and dermal  
880 irritation potential of surfactants. *Food and Chemical Toxicology* 45(5):747-58. doi:  
881 10.1016/j.fct.2006.10.024.
- 882 Melik-Parsadaniantz, S., Rostène, W., Baudouin, C., & Réaux-Le Goazigo, A. (2018).  
883 Understanding chronic ocular pain. *Biologie Aujourd'hui*, 212(1-2):1-11. French. doi:  
884 10.1051/jbio/2018017.
- 885 Murphy, P., Kabir, M.H., Srivastava, T., Mason, M.E., Dewi, C.U., Lim, S., ... O'Connor,  
886 M.D. (2018). Light-focusing human micro-lenses generated from pluripotent stem cells  
887 model lens development and drug-induced cataract in vitro. *Development*,  
888 145(1):dev155838. doi: 10.1242/dev.155838.
- 889 Narda, M., Ramos-Lopez, D., Mun, G., Valderas-Martinez, P., & Granger, C. (2019). Three-  
890 tier testing approach for optimal ocular tolerance sunscreen. *Cutaneous and Ocular  
891 Toxicology*, 38(3):212-220. doi: 10.1080/15569527.2019.1601106
- 892 OECD (2012) "Draft OECD Guideline: The Cytosensor Microphysiometer Test Method: An  
893 in Vitro Method for Identifying Ocular Corrosive and Severe Irritant Chemicals as Well  
894 as Chemicals Not Classified as Ocular Irritants". OECD Publishing, Paris.

895 OECD (2017) "Test No. 460: Fluorescein Leakage Test Method for Identifying Ocular  
896 Corrosives and Severe Irritants". OECD Publishing, Paris.

897 OECD (2018a) "Test No. 438: Isolated Chicken Eye Test Method for Identifying i) Chemicals  
898 Inducing Serious Eye Damage and ii) Chemicals Not Requiring Classification for Eye  
899 Irritation or Serious Eye Damage". OECD Publishing, Paris.

900 OECD (2018b) "Guidance Document No. 160: Collection of Tissues for Histological  
901 Evaluation and Collection of Data on Non-Severe Irritants". OECD Publishing, Paris.

902 OECD (2019a) "Test No. 492: Reconstructed Human Cornea-like Epithelium (RhCE) Test  
903 Method for Identifying Chemicals Not Requiring Classification and Labelling for Eye  
904 Irritation or Serious Eye Damage". OECD Publishing, Paris.

905 OECD (2019b) "Guidance Document No. 263: Guidance Document on an Integrated  
906 Approach on Testing and Assessment (IATA) for Serious Eye Damage and Eye  
907 Irritation". OECD Publishing, Paris.

908 OECD (2019c) "Test No. 494: Vitrigel-Eye Irritancy Test Method for Identifying Chemicals  
909 Not Requiring Classification and Labelling for Eye Irritation or Serious Eye Damage".  
910 OECD Publishing, Paris.

911 OECD (2019d). Test No. 496: In Vitro Macromolecular Test Method for Identifying  
912 Chemicals Inducing Serious Eye Damage and Chemicals Not Requiring Classification  
913 for Eye Irritation or Serious Eye Damage". OECD Publishing, Paris.

914 OECD (2020a) "Test No. 405: Acute Eye Irritation/Corrosion". OECD Publishing, Paris.

915 OECD (2020b) "Test No. 437: Bovine Corneal Opacity and Permeability Test Method for  
916 Identifying i) Chemicals Inducing Serious Eye Damage and ii) Chemicals Not Requiring  
917 Classification for Eye Irritation or Serious Eye Damage". OECD Publishing, Paris.

918 OECD (2020c) "Test No. 491: Short Time Exposure In Vitro Test Method for Identifying i)  
919 Chemicals Inducing Serious Eye Damage and ii) Chemicals Not Requiring Classification  
920 for Eye Irritation or Serious Eye Damage". OECD Publishing, Paris.

921 OECD (2020d). *The OECD QSAR Toolbox*. [Internet][cited 2020 jun 27]. Available from:  
922 <http://www.oecd.org/chemicalsafety/risk-assessment/oecd-qsar-toolbox.htm>

923 OECD (2021) "Guideline No.497: Guideline on Defined Approaches for Skin  
924 Sensitisation". OECD Publishing, Paris.

925 OECD Webinar (2019a) *OECD Alternatives to in Vivo Eye Irritation Testing*. [Internet][cited  
926 2020 apr 23]. Available from: <https://www.youtube.com/watch?v=IVBXooZCtf>

927 OECD Webinar (2019b) *Testing and Assessment Methodologies: Adverse Outcome Pathway  
928 (AOP) Framework*. [Internet][cited 2020 apr 24]. Available from:  
929 <https://www.youtube.com/watch?v=qyrCC-Kxcik> (April 24, 2020).

930 Pak, J., Chen, Z.J., Sun, K., Przekwas, A., Walenga, R., & Fan, J. (2018). Computational  
931 modeling of drug transport across the in vitro cornea. *Computers in Biology and  
932 Medicine*, 92:139-146. doi: 10.1016/j.compbiomed.2017.11.009.

933 Pape, W.J., Pfannenbecker, U., & Hoppe, U. (1987-1988). Validation of the red blood cell test  
934 system as in vitro assay for the rapid screening of irritation potential of surfactants.  
935 *Molecular Toxicology*, 1(4):525-36.

936 Pape, W.J., & Hoppe, U. (1990). Standardization of an in vitro red blood cell test for

- 937 evaluating the acute cytotoxic potential of tensides. *Arzneimittelforschung*, 40(4):498-  
938 502.
- 939 Pauly, A., Meloni, M., Brignole-Baudouin, F., Warnet, J.M., & Baudouin, C. (2009). Multiple  
940 endpoint analysis of the 3D-reconstituted corneal epithelium after treatment with  
941 benzalkonium chloride: early detection of toxic damage. *Investigative Ophthalmology &*  
942 *Visual Science*, 50(4):1644-52. doi: 10.1167/iovs.08-2992.
- 943 Petit, J.Y., Doré, V., Marignac, G., & Perrot, S. (2017). Assessment of ocular discomfort  
944 caused by 5 shampoos using the Slug Mucosal Irritation test. *Toxicology In Vitro*,  
945 40:243-247. doi: 10.1016/j.tiv.2017.01.002.
- 946 Piehl, M., Carathers, M., Soda, R., Cerven, D., & DeGeorge, G. (2011). Porcine Corneal  
947 Ocular Reversibility Assay (PorCORA) predicts ocular damage and recovery for global  
948 regulatory agency hazard categories. *Toxicology In Vitro*, 25(8):1912-8. doi:  
949 10.1016/j.tiv.2011.06.008.
- 950 Prinsen, M.K., & Koëter, H.B. (1993). Justification of the enucleated eye test with eyes of  
951 slaughterhouse animals as an alternative to the Draize eye irritation test with rabbits.  
952 *Food and Chemical Toxicology*, 31(1):69-76. doi: 10.1016/0278-6915(93)90182-x.
- 953 Sarkar, J., Chaudhary, S., Namavari, A., Ozturk, O., Chang, J.H., Yco, L., ... Jain, S. (2012).  
954 Corneal neurotoxicity due to topical benzalkonium chloride. *Investigative*  
955 *Ophthalmology & Visual Science*, 53(4):1792-802. doi: 10.1167/iovs.11-8775.
- 956 Schrage, N., Frentz, M., & Spoeler, F. (2012). The Ex Vivo Eye Irritation Test (EVEIT) in  
957 evaluation of artificial tears: Purite-preserved versus unpreserved eye drops. *Graefes*  
958 *Archive For Clinical and Experimental Ophthalmology*, 250(9):1333-40. doi:  
959 10.1007/s00417-012-1999-3.
- 960 Seo, J., Byun, W.Y., Alisafaei, F., Georgescu, A., Yi, Y.S., Massaro-Giordano, M., ... Huh,  
961 D. (2019). Multiscale reverse engineering of the human ocular surface. *Nature Medicine*,  
962 25(8):1310-1318. doi: 10.1038/s41591-019-0531-2.
- 963 Sharif, R., Priyadarsini, S., Rowsey, T.G., Ma, J.X., & Karamichos, D. (2018). Corneal Tissue  
964 Engineering: An In Vitro Model of the Stromal-nerve Interactions of the Human Cornea.  
965 *Journal of Visualized Experiments*, (131):56308. doi: 10.3791/56308.
- 966 Sosa-Hernández, J.E., Villalba-Rodríguez, A.M., Romero-Castillo, K.D., Aguilar-Aguila-  
967 Isaías, M.A., García-Reyes, I.E., Hernández-Antonio, A., ... Iqbal, H.M.N. (2018).  
968 Organs-on-a-Chip Module: A Review from the Development and Applications  
969 Perspective. *Micromachines (Basel)*, 9(10):536. doi: 10.3390/mi9100536.
- 970 Spielmann, H. (2014). International Regulation of Toxicological Test Systems. In F.-X.  
971 Reichl & M. Schwenk (Eds.), *Regulatory Toxicology* (pp. 181–189). Springer Berlin  
972 Heidelberg. [https://doi.org/10.1007/978-3-642-35374-1\\_41](https://doi.org/10.1007/978-3-642-35374-1_41)
- 973 Spöler, F., Kray, O., Kray, S., Panfil, C., & Schrage, N.F. (2015). The Ex Vivo Eye Irritation  
974 Test as an alternative test method for serious eye damage/eye irritation. *Alternative to*  
975 *Laboratory Animals*, 43(3):163-79. doi: 10.1177/026119291504300306.
- 976 Srinivasan, B., Kolli, A.R., Esch, M.B., Abaci, H.E., Shuler, M.L., & Hickman, J.J. (2015).  
977 TEER measurement techniques for in vitro barrier model systems. *Journal of Laboratory*  
978 *Automation*, 20(2):107-26. doi: 10.1177/2211068214561025.
- 979 Susaimanickam, P.J., Maddileti, S., Pulimamidi, V.K., Boyinpally, S.R., Naik, R.R., Naik,  
980 M.N.,... Mariappan, I. (2017). Generating minicorneal organoids from human induced

- 981 pluripotent stem cells. *Development*, 144(13):2338-2351. doi: 10.1242/dev.143040.
- 982 Takezawa, T., Ozaki, K., Nitani, A., Takabayashi, C., & Shimo-Oka, T. (2004). Collagen  
983 vitrigel: a novel scaffold that can facilitate a three-dimensional culture for reconstructing  
984 organoids. *Cell Transplantation*, 13(4):463-73. doi: 10.3727/000000004783983882.
- 985 Tandon, R., Bartok, M., Zorn-Kruppa, M., Brandner, J.M., Gabel, D., & Engelke, M. (2015).  
986 Assessment of the eye irritation potential of chemicals: A comparison study between two  
987 test methods based on human 3D hemi-cornea models. *Toxicology In Vitro*, 30(1 Pt  
988 B):561-8. doi: 10.1016/j.tiv.2015.09.003.
- 989 Vij, P., Carathers, M., Yasso, B., & Varsho, B. (2017). *Resolving Severe/Corrosive Irritant*  
990 *Ocular Classifications Using an Alternative Dual Ex Vivo Assay System*. [Internet][cited  
991 2020 dec 20]. Available from: <http://www.mbresearch.com/pdfs/10WC/PorCORA> and  
992 [BCOP.pdf](http://www.mbresearch.com/pdfs/10WC/BCOP.pdf)
- 993 Russell, W.S.M., & Burch, R.L. (1959). *The Principles of Humane Experimental Technique*.  
994 London: Methuen.
- 995 Wang, S., Ghezzi, C.E., Gomes, R., Pollard, R.E., Funderburgh, J.L., & Kaplan, D.L. (2017).  
996 In vitro 3D corneal tissue model with epithelium, stroma, and innervation.  
997 *Biomaterials*, 112:1-9. doi: 10.1016/j.biomaterials.2016.09.030.
- 998 Wilson, S.L., Ahearne, M., & Hopkinson, A. (2015). An overview of current techniques for  
999 ocular toxicity testing. *Toxicology*, 327:32-46. doi: 10.1016/j.tox.2014.11.003.
- 1000 Yamaguchi, H., Kojima, H., & Takezawa, T. (2016). Predictive performance of the Vitrigel-  
1001 eye irritancy test method using 118 chemicals. *Journal of Applied Toxicology*,  
1002 36(8):1025-37. doi: 10.1002/jat.3254.
- 1003 Yang, C., Yang, Y., Brennan, L., Bouhassira, E.E., Kantorow, M., & Cvekl, A. (2010).  
1004 Efficient generation of lens progenitor cells and lentoid bodies from human embryonic  
1005 stem cells in chemically defined conditions. *FASEB Journal*, 24(9):3274-83. doi:  
1006 10.1096/fj.10-157255.
- 1007 Zhong, X., Gutierrez, C., Xue, T., Hampton, C., Vergara, M.N., Cao, H., ... Canto-Soler,  
1008 M.V. (2014). Generation of three-dimensional retinal tissue with functional  
1009 photoreceptors from human iPSCs. *Nature Communication*, 5:4047. doi:  
1010 10.1038/ncomms5047.
- 1011 Zorn-Kruppa, M., Houdek, P., Wladykowski, E., Engelke, M., Bartok, M., Mewes, K.R., ...  
1012 Brandner, J.M. (2014). Determining the Depth of Injury in Bioengineered Tissue Models  
1013 of Cornea and Conjunctiva for the Prediction of All Three Ocular GHS Categories. *PLoS*  
1014 *One*, 9(12):e114181. doi: 10.1371/journal.pone.0114181.
- 1015 Zuang, V. (2001). The neutral red release assay: a review. *Alternative to Laboratory Animals*,  
1016 29(5):575-99. doi: 10.1177/026119290102900513.

1017

1018

1019

1020

1021 **Tables**

1022 **Table I. Summary of models validated or under evaluation by the OECD.** \*Values given  
1023 in OECD GL to identify Category 1 or not-classified substances (depending on assay  
1024 applicability) in comparison to the Draize eye irritation test.

1025 **Table II. Summary of validated RhCE models for ocular irritation according to OECD**  
1026 **GL 492.**

1027 **Table III – Summary of innovative models with potential for evaluation of ocular**  
1028 **surface toxicity.**

1029

## 1030 **Figures**

1031 **Figure 1. Schematic presentation of the matrix created in the Red Blood Cell test and**  
1032 **the principle of denaturation** (modified from OECD Webinar 2019a)

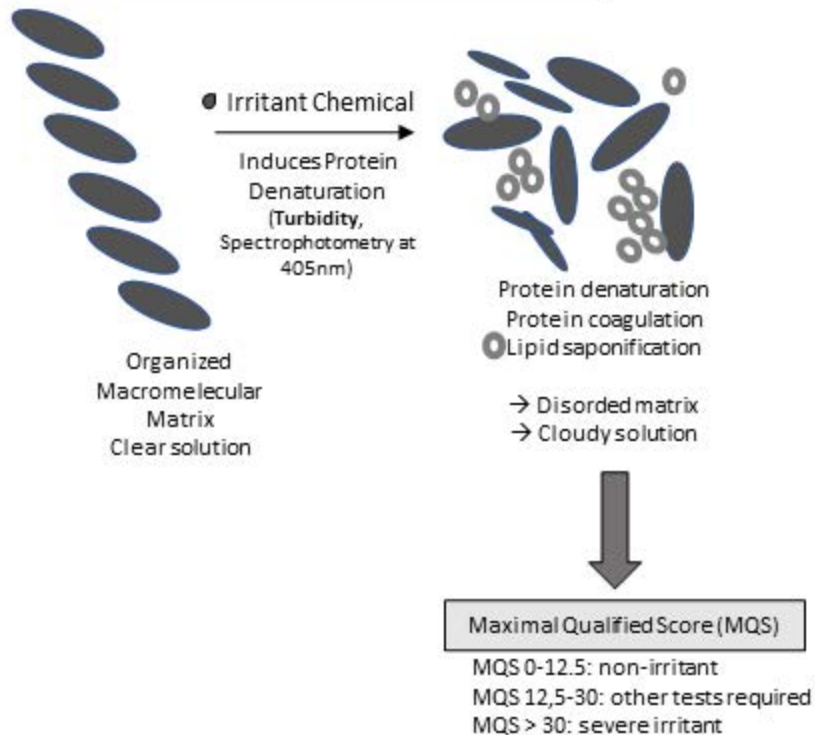
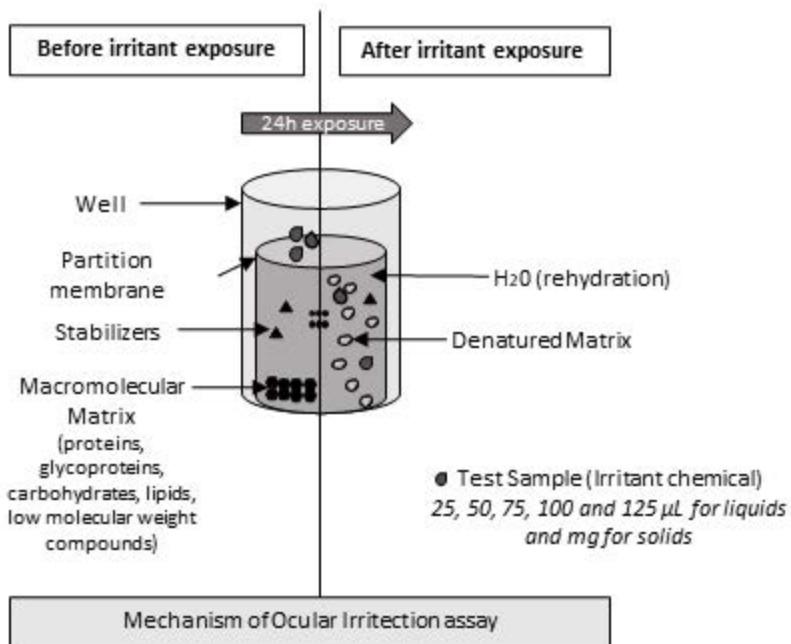
1033 **Figure 2. Procedure to prepare the embryonated egg in the HET-CAM testing method**  
1034 (personal images, not published)

1035 **Figure 3. Schematic evaluation protocol for ocular discomfort in the slug irritation**  
1036 **model** (modified from Lenoir *et al.* 2011). *CP: Contact Period; SIB: Stinging, Itching and*  
1037 *Burning*

1038 **Figure 4. Schematic representation of the coculture established** between conjunctival  
1039 epithelial cells and lacrimal spheroids (modified from Lu *et al.* 2017).

1040 **Figure 5. Schematic comparison of human corneal structure with 3D triculture model**  
1041 **structure** (modified from Wang *et al.* 2017).

1042





Egg shell opening with the tip of pliers after spotting the air compartment by transparency

Enlargement of the opening with scissors

Access to the membranes

Addition of NaCl 0.9% to separate the protective membrane from the vascularized membrane

NaCl 0.9% removal

Protective membrane removal

Access to the vascularized membrane, beginning of eye irritation test



**Egg opening procedure**

**Exposure to test compound**

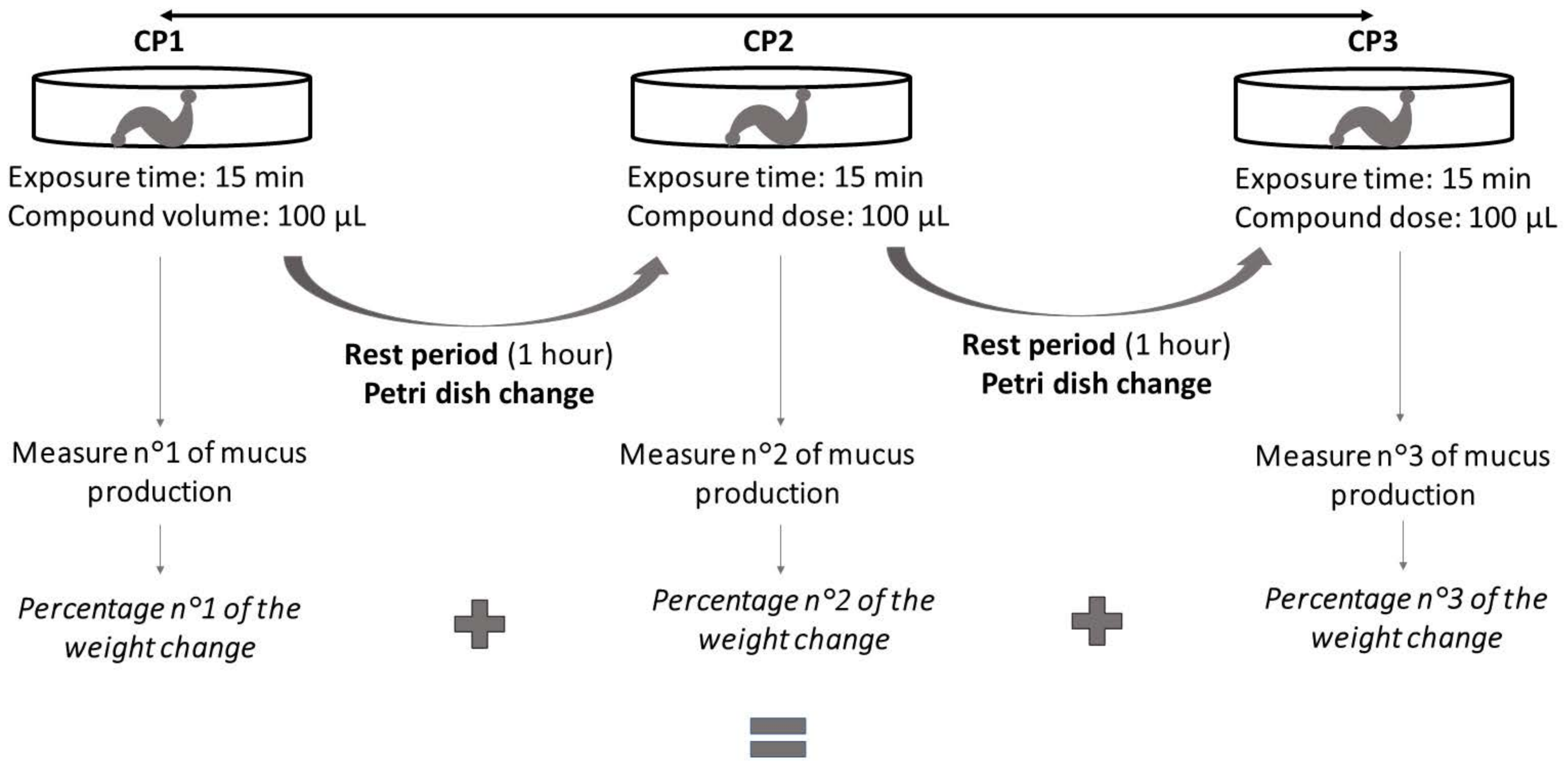
HET-CAM: 30 sec, 2, 5 min

CAMVA: 30 min

**Irritation Score, IS**

- hemorrhage appearance time,
- vessel lysis appearance time,
- protein coagulation apparition time

Conducted over a 24-hour period



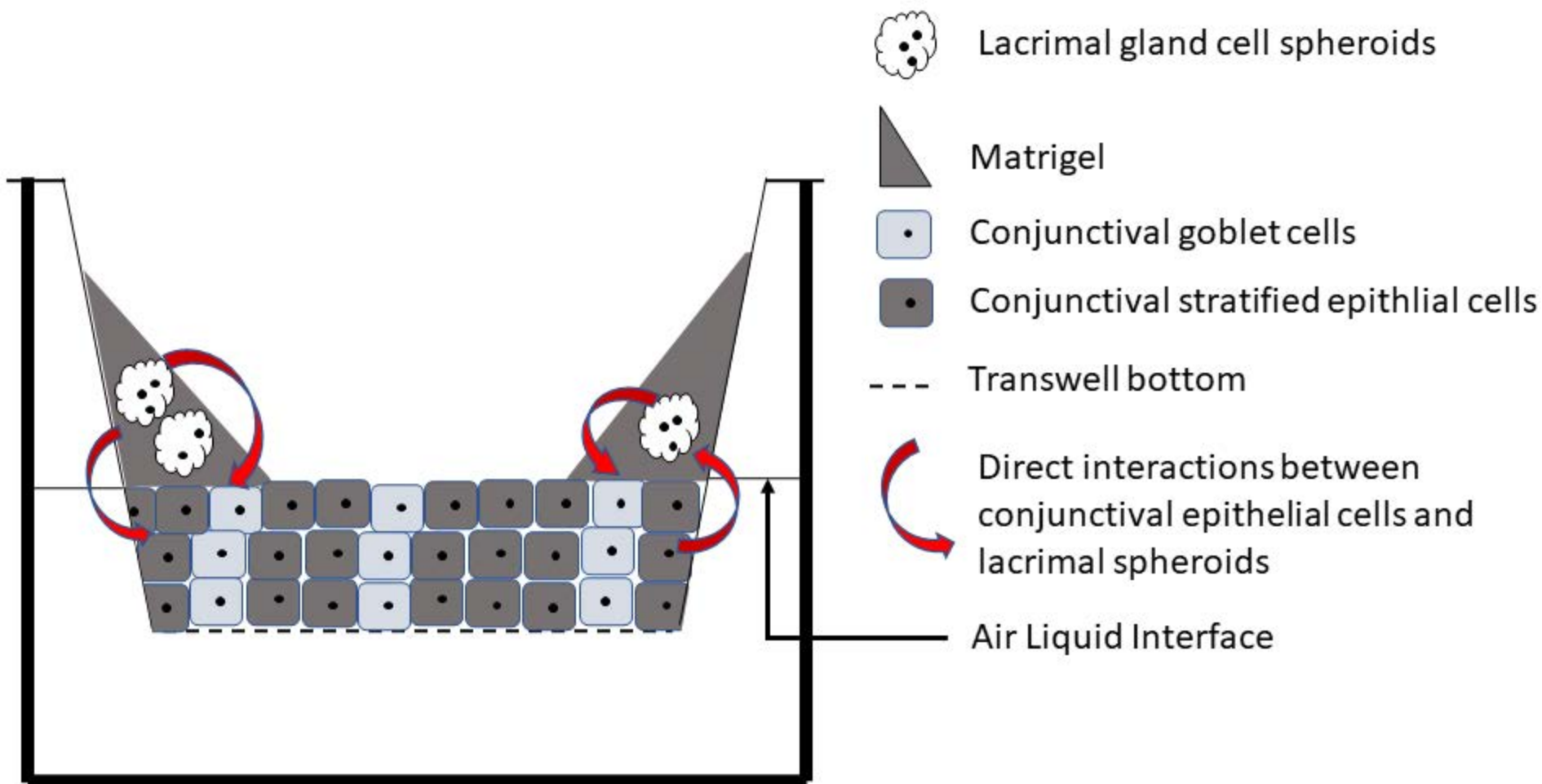
Legends:

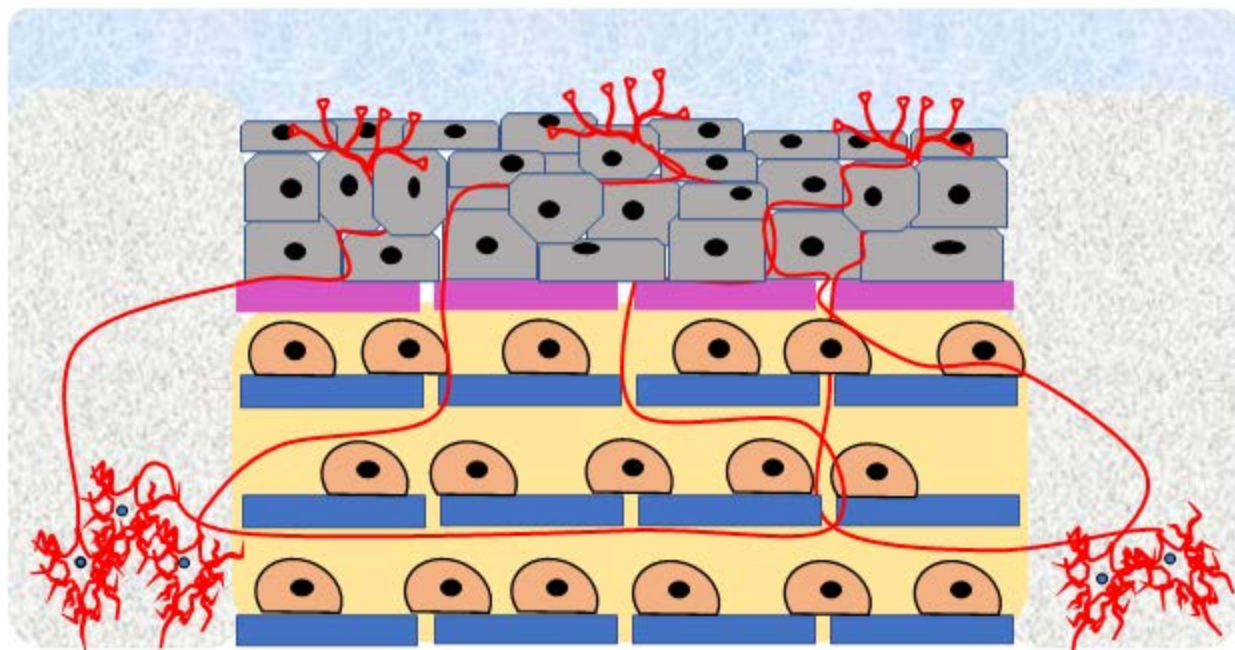
 Petri dish

 Slug





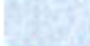


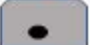

\*SIB : stinging, itching and/or burning

**Light SIB\* = 3 to 8%**  
**Moderate SIB\* = 8 to 15%**  
**Severe SIB\* > 15%**





### Legends

-  *stamped porous silk film for epithelium and stroma development*
-  *porous patterned silk films for neuronal growth stimulation*
-  *silk sponge for corneal rigidity*
-  *collagen hydrogel (containing NGF) for neuronal growth stimulation*
-  *air liquid interface (ALI) to improve triculture phenotype*
-  *chicken Dorsal Root Ganglion (DRG) cell body*  
*DRG axons*
-  *DRG nerve ending*
-  *human primary corneal cells*
-  *human corneal stromal stem cells*



Ocular irritation tests	Draize test	RhCE	BCOP	ICE	Fluorescein Leakage	STE	Vitrigel EIT	Ocular Irritection®	IRE	HET-CAM / CAMVA	CM	NRR	RBC
OECD guideline (last update)	OECD GL 405 (2020)	OECD GL 492 (2019)	OECD GL 437 (2020)	OECD GL 438 (2018)	OECD GL 460 (2017)	OECD GL 491 (2020)	OECD GL 494 (2019)	OECD GL 496 (2019)	Not validated	Not validated	Temporary version released in 2012 (development discontinued in 2016)	Not validated	Not validated
Model	<i>In vivo</i> , albino rabbit	<i>In vitro</i> , 3D human reconstructed epithelium	<i>Ex Vivo</i> , isolated bovine cornea	<i>Ex Vivo</i> , enucleated chicken eye	<i>In vitro</i> , tubular kidney MDCK CB997 cell line, monolayer, semi-permeable membrane	<i>In vitro</i> , monolayer confluent rabbit corneal fibroblasts (ex. CCL60 cell line)	<i>In vitro</i> , human reconstructed epithelium (Vitrigel matrix)	<i>In vitro</i> , acellular system, macro-molecular matrix (proteins, lipids, carbohydrates,...)	<i>Ex vivo</i> , enucleated rabbit eye	Chorioallantoic Membrane of chicken embryo egg	<i>In vitro</i> , mono-layer mice fibroblasts from L929 cell line cultivated on a polycarbonate insert	<i>In vitro</i> , mono-layer of 3T3-L1 fibroblasts or NHEK human keratinocytes (FRAME/ Clonetic protocol)	Isolated red blood cells
Recommended strategy	Last resort (forbidden for cosmetics)	Bottom-Up	Bottom-Up, Top-Down	Bottom-Up, Top-Down	Top-Down	Bottom-Up, Top-Down	Bottom-Up	Bottom-Up, Top-Down	Not recommended	Not recommended	(If validation of GL: Bottom-Up, Top-Down)	Not recommended (supplementary data required)	Not recommended (supplementary data required)
Field of applicability	Liquids, solids, aerosols	Liquids, semi-solids, solids, waxes	Liquids, semi-solids, creams, waxes (including surfactants)	Substances and mixtures	Water-soluble substances and mixtures	All types of products (except volatile substances, non surfactant products)	Chemical products with pH > 5, including volatile or coloured compounds (excluding solids)	Solids and liquids with 4 ≤ pH ≤ 9	Substances and mixtures	Substances and mixtures	Water-soluble compounds (including mixtures), solids/viscous substances / uniform suspensions	Water-soluble substances	Substances and mixtures
GSH categories	1, 2A, 2B, not-classified	Not-classified (in process of validation to distinguish 1, 2A et 2B with EpiOcular® time-to-toxicity assay)	1, not-classified	1, not-classified	1	1, not-classified	not-classified	1, not-classified	(accepted in European Union for category 1)	HET-CAM accepted in European Union for category 1	1, not-classified	not-classified	1, not-classified
Compound exposure time	21 days	See Table 2	10 min (other exposure times if scientific rationale)	10 sec (rinsing removal)	1 min (followed by a 30min incubation of fluorescein)	5 min (two concentrations, 0.5% and 0.05%)	3 min	24h (5 concentrations, 25, 50, 75, 100, 125 µL or µg)	10 sec (rinsing removal)	30 sec, 2, 5 min (HET-CAM) / 30 min (CAMVA)	810 sec (= 13, 5min, followed by a 6 min wash out cycle)	1 or 5 min (FRAME or Clonetic protocol)	10 min to 1 hour at room temperature (under continuous stirring)
Endpoints	<b>Conjunctiva</b> (chemosis, redness, tearing), <b>Corneal</b> opacification, <b>Iris</b> (swelling, light reactivity)	Mitochondrial metabolic capacity	Corneal opacity; Fluorescein retention	Corneal opacity; Fluorescein retention; Morphological alteration (evaluated after 30 min, 1, 2, 3, and 4 hours of product retrieval)	Fluorescein diffusion (spectrophotometry at 530 nm)	Mitochondrial metabolic capacity	TEER (measured every 10 s during 3 min)	Turbidity variations (spectrophotometry at 405 nm)	Corneal opacity, edema; Fluorescein penetration; Epithelial changes (evaluated after 30 min, 1, 2, 3, and 4 hours of product retrieval)	Hemorrhage / vessel lysis / protein coagulation apparition times	Dose-response study, pH changes evaluation over time	Dose-response study, Release of preloaded neutral red, 3 hours before exposure (spectrophotometry at 546-550 nm)	Hemoglobin leakage (photometry at 540 nm); Oxyhemoglobin denaturation (spectrophotometry at 575 nm)
Threshold or Score	Maximal ocular irritation ( <b>Max.O.I</b> )	MTT or WST threshold (see table 2)	<i>In Vitro</i> Irritancy Score ( <b>IVIS</b> )	Addition of scores for each endpoint graded from I to IV	Fluorescein Leakage of 20% ( <b>FL<sub>20%</sub></b> )	MTT threshold	Score that combines time lag, intensity and plateau level	Maximal Qualified Score ( <b>MQS</b> )	Addition of scores for each endpoint	Irritation Score ( <b>IS</b> )	Metabolic Rate Decrement of 50% ( <b>MRD<sub>50</sub></b> )	Neutral Red Release of 50% ( <b>NRR<sub>50</sub></b> )	ratio concentration inducing a red cell hemolysis of 50% / Denaturation index ( <b>H<sub>50</sub>/DI</b> )



Ocular irritation tests	Draize test	RhCE	BCOP	ICE	Fluoresceine Leakage	STE	Vitrigel EIT	Ocular Irritection®	IRE	HET-CAM / CAMVA	CM	NRR	RBC
<b>Accuracy *</b>	Reference	EpiOcular™, 80% (96/112) SkinEthic™ HCE, 84% (168/200)	79% (150/191)	83% (142/172)	77% (117/151)	83% (120/140)	78% (73/93)	74% (65/88)	78% (110/141)	69% (41/59)	Data not found	Variable, protocol dependent	96.7% (Alves et al. 2008)
<b>Specificity *</b>	Reference	EpiOcular™, 37% (21/55) SkinEthic™ HCE, 28% (29/103)	25% (32/126)	7% (9/127)	7% (7/103)	1% (1/86)	70% (23/33)	81% (55/68)	6% (4/62)	64% (18/28)	2% (1/48)	Variable, protocol dependent	100% (Alves et al. 2008)
<b>Sensitivity *</b>	Reference	EpiOcular™, 4% (3/57) SkinEthic™ HCE, 5% (5/97)	14% (9/65)	47% (21/45)	56% (27/48)	51% (20/39)	83% (50/60)	50% (10/20)	34% (27/79)	0% (0/31)	20.5% (7/34)	Variable, protocol dependent	91.6% (Alves et al. 2008)
<b>Main limits</b>	<ul style="list-style-type: none"> <li>- 3R rule ethical problem</li> <li>- Forbidden for cosmetics</li> <li>- Inter/Intra laboratory variability</li> <li>- Over-estimation of toxicities occurring in humans</li> </ul>	<ul style="list-style-type: none"> <li>- No toxicity evaluation of eyelid, iris, and other ocular structures</li> <li>- No evaluation of gas and aerosols</li> </ul>	<ul style="list-style-type: none"> <li>- No toxicity evaluation of eyelid, iris, etc</li> <li>- No evaluation of gas and aerosols               <ul style="list-style-type: none"> <li>- Over-estimation for pour alcohols, ketones</li> </ul> </li> </ul>	<ul style="list-style-type: none"> <li>- No toxicity evaluation of eyelid, iris, and other ocular structures</li> <li>- No evaluation of gas and aerosols</li> </ul>	<ul style="list-style-type: none"> <li>- No toxicity evaluation of eyelid, iris, and other ocular structures</li> <li>- No evaluation of gas and aerosols</li> </ul>	<ul style="list-style-type: none"> <li>- No toxicity evaluation of eyelid, iris, and other ocular structures</li> <li>- No evaluation of gas and aerosols</li> </ul>	<ul style="list-style-type: none"> <li>- No toxicity evaluation of eyelid, iris, and other ocular structures</li> <li>- No evaluation of gas and aerosols</li> </ul>	<ul style="list-style-type: none"> <li>- No cytotoxicity evaluation</li> <li>- Reduced field of applicability</li> </ul>	<ul style="list-style-type: none"> <li>- No standardized protocol,</li> <li>- No sufficient data on decision criteria and on inter-laboratory reproducibility</li> </ul>	<ul style="list-style-type: none"> <li>- No standardized protocol</li> <li>- Embryo egg can be considered as animal experimentation depending on countries</li> </ul>	<ul style="list-style-type: none"> <li>- No evaluation of gas and aerosols</li> </ul>	<ul style="list-style-type: none"> <li>- No sufficient data on inter-laboratory reproducibility</li> <li>- Reduced field of applicability (supplementary data needed)</li> </ul>	<ul style="list-style-type: none"> <li>- No sufficient data on field of applicability</li> </ul>



OECD GL 492		EpiOcular™	SkinEthic™ HCE	LabCyte CORNEA-MODEL24	MCTT HCE™
Cell type		Primary human keratinocytes from human epiderma	Immortalized human corneal epithelial cells	Primary human corneal epithelial cells	Primary human corneal epithelial cells
Field of applicability		Solids, liquids, semi-solids and waxes			
Validated Reference Methods (VRM)		MRV1	MRV2	/	/
3D development*		At least three viable cell layers and of a non keratinized surface	At least four viable cell layers that include basal columnar cells, transitory amplifier cells and squamous superficial cells	At least three viable cell layers and of a non keratinized surface	At least three viable cell layers and of a non keratinized surface
Compound exposure time	Liquids	30 min	30 min	1 min	10 min
	Solids <i>(or liquids non applicable with a pipette)</i>	6 hours	4 hours	24 hours	3 hours
Cytotoxicity test** (Non irritant threshold)		MTT (> 60 %)	MTT (>50%)	WST-8 (>40%)	WST-8 (> 35% for liquids; > 60% for solids)

\* The barrier function of the 3D reconstructed-cornea epithelia must be validated based on their ability to resist penetration by cytotoxic compounds such as Triton X-100 and sodium dodecylsulfate.

\*\* The two colorimetric tests, MTT (3-(4,5-dimethylthiazol-2-yl)-2,5-diphenyltetrazolium bromide) and WST (water-soluble tetrazolium salts)-8 tests are similar. In the first one, formazan is formed intracellularly, requiring the step of cell lysis with isopropanol before the absorbance measurement, while in the second one, formazan is present directly in the cell culture medium. This colorimetric measure is proportional to the number of live cells (Pauly et al. 2009).

	Multicellular 3D models			Models on-a-chip				Organoids	
	Coculture conjunctiva / lacrimal glands	Coculture SH-SY5Y neurons / stromal corneal cells on an insert	Tri-culture neurons / epithelial cells / stromal cells	Cornea-on-a-chip, lacrimal flows	Cornea-on-a-chip and shear stress	Coculture on-a-chip cornea – conjunctiva	Compartmentalized corneal neurones	Cornea	Lens
Cell types	<ul style="list-style-type: none"> <li>Primary epithelial conjunctival rabbit cells</li> <li>Primary rabbit acinous lacrimal glands spheroids</li> </ul>	<ul style="list-style-type: none"> <li>Primary human corneal fibroblasts</li> <li>Human neuroblastoma SH-SY5Y cell line</li> </ul>	<ul style="list-style-type: none"> <li>HCE human corneal epithelial cell line</li> <li>Stromal human stem cells (hCSCCs)</li> <li>Neuronal cells (DRG)</li> </ul>	<ul style="list-style-type: none"> <li>HCE human corneal epithelial cell line</li> </ul>	<ul style="list-style-type: none"> <li>HCE human corneal epithelial cell line</li> <li>Or</li> <li>Primary mice epithelial and endothelial corneal cells</li> </ul>	<ul style="list-style-type: none"> <li>Primary human corneal epithelial cells</li> <li>Human immortalized conjunctival cells</li> </ul>	<ul style="list-style-type: none"> <li>Primary trigeminal ganglion mice cells (<i>model improvement possible by adding epithelial corneal cell to form a coculture</i>)</li> </ul>	<ul style="list-style-type: none"> <li>IMR90.4 iPS cell line</li> </ul>	<ul style="list-style-type: none"> <li>human pluripotent embryonic stem cells (hESC line CA1)</li> </ul>
Advantages	<ul style="list-style-type: none"> <li>Production of aqueous and mucinic lacrimal layers</li> </ul>	<ul style="list-style-type: none"> <li>Production <i>de novo</i> of extracellular matrix by fibroblasts</li> <li>Mimic the interactions of nerves with the stroma</li> </ul>	<ul style="list-style-type: none"> <li>Air liquid interface culture on silk protein to better mimic mechanical corneal properties and improve neuronal development</li> </ul>	<ul style="list-style-type: none"> <li>Mimic pulsatile flow generated by eyelid blinking</li> <li>Mimic continuous flow generated by lacrimal secretion</li> </ul>	<ul style="list-style-type: none"> <li>Mimic lacrimal flow generated by eye blinking (bidirectional flow)</li> <li>Mimic aqueous humour evacuation through Schlemm’s canal (unidirectional flow)</li> </ul>	<ul style="list-style-type: none"> <li>Mimic stroma through collagen matrix</li> <li>Mimic lacrimal flow through a perfusion system</li> <li>Mimic eyelid blinking through biomimetic system</li> </ul>	<ul style="list-style-type: none"> <li>Separate nerve endings (distal compartment) from neuronal cell bodies (proximal compartment) to better mimic physiology and independently evaluate the impact of a toxic on nerve endings</li> </ul>	<ul style="list-style-type: none"> <li>Lamellar structure of the cornea (epithelium, stroma, endothelium) identifiable at 30 days of culture</li> </ul>	<ul style="list-style-type: none"> <li>Formation of a fibrillary structure characteristic of the lens</li> </ul>
Evaluated parameters	<ul style="list-style-type: none"> <li>Permeability of tight junctions (conjunctival epithelium) to dextran</li> <li>Lacrimal fluid thickness</li> <li>Epithelial gene marker (KRT4)</li> <li>Mucin gene marker / production (MUC5AC)</li> <li>Inflammatory gene marker (IL-1<math>\beta</math>, MMPs)</li> </ul>	<ul style="list-style-type: none"> <li>Collagen and fibrosis gene markers (alpha-SMA)</li> <li>Structural changes (transmission electron microscopy)</li> <li>Neuronal activation markers (cFOS, TRPV1, TRPM8, <i>etc</i>)</li> </ul>	<ul style="list-style-type: none"> <li>Cell viability (LIVE/DEAD Viability/ Cytotoxicity Kit)</li> <li>Corneal epithelium and stromal phenotype (involucrin, KRT3, connexin 37, ALDH3A1)</li> </ul>	<ul style="list-style-type: none"> <li>Epithelium thickness</li> <li>Corneal epithelium phenotype (ZO-1)</li> <li>Membrane permeability (TEER)</li> </ul>	<ul style="list-style-type: none"> <li>Epithelium thickness</li> <li>Epithelial permeability (fluorescein, dextran)</li> <li>Corneal epithelium phenotype (ZO-1, KRT19, KRT12)</li> </ul>	<ul style="list-style-type: none"> <li>Epithelium thickness</li> <li>Corneal epithelium phenotype (p63, KRT19, KRT3)</li> <li>Lacrimal film thickness</li> <li>Inflammatory cytokines production (IL-<math>\beta</math>, TNF-<math>\alpha</math>) and metalloproteinases (MMP-9)</li> </ul>	<ul style="list-style-type: none"> <li>Inflammatory markers</li> <li>Cell death markers</li> <li>Morphological alterations of axons (CFSE coloration)</li> </ul>	<ul style="list-style-type: none"> <li>Lamellar structure thickness</li> <li>Corneal epithelium phenotype (KRT3, KRT14, p63<math>\alpha</math>, KERA, type I / V / VIII collagen, LUM)</li> <li>Organization of collagen fibrils (transmission electron microscopy)</li> </ul>	<ul style="list-style-type: none"> <li>Lens phenotype (ROR, crystallines <math>\alpha</math> et <math>\beta</math>, integrins, laminins et collagens)</li> <li>Light focusing ability</li> </ul>
References	Lu <i>et al.</i> 2017	Sharif <i>et al.</i> 2018	Wang <i>et al.</i> 2015 Wang <i>et al.</i> 2017	Bennet <i>et al.</i> 2018	Abdalkader and Kamei 2018 Bai <i>et al.</i> 2020	Seo <i>et al.</i> 2019	Vitoux <i>et al.</i> 2020	Foster <i>et al.</i> 2017 Susaimanickam <i>et al.</i> 2017 Foster <i>et al.</i> 2020	Murphy <i>et al.</i> 2018